

ONE DIMENSIONAL BANDSTRUCTURE CALCULATIONS

by

Norman Gabriel Hall

A thesis
presented to the University of Manitoba
in partial fulfillment of the
requirements for the degree of
Master of Science
in
Physics

Winnipeg, Manitoba

(c) Norman Gabriel Hall, 1984

ONE DIMENSIONAL BAND STRUCTURE CALCULATIONS.

by

Norman Gabriel Hall

A thesis submitted to the Faculty of Graduate Studies of
the University of Manitoba in partial fulfillment of the requirements
of the degree of

MASTER OF SCIENCE

© 1984

Permission has been granted to the LIBRARY OF THE UNIVERSITY OF MANITOBA to lend or sell copies of this thesis, to the NATIONAL LIBRARY OF CANADA to microfilm this thesis and to lend or sell copies of the film, and UNIVERSITY MICROFILMS to publish an abstract of this thesis.

The author reserves other publication rights, and neither the thesis nor extensive extracts from it may be printed or otherwise reproduced without the author's written permission.

ABSTRACT

One-electron energy bands in a one-dimensional crystal lattice are studied. Bound and ionized regions of the crystal are studied, the latter exhibiting vanishing gaps for certain potentials. Physical criteria for the existence of gaps are discussed. Electronic Charge Densities are also presented.

ACKNOWLEDGEMENTS

Dr. P.D. Loly supervised this project.

CONTENTS

ABSTRACT	iv
ACKNOWLEDGEMENTS	v
<u>Chapter</u>		<u>page</u>
I.	INTRODUCTION	1
II.	SOME METHODS OF ONE-DIMENSIONAL BANDSTRUCTURE CALCULATIONS	4
III.	PWD METHOD	8
	Computer coding of problem	13
	Initialization	14
	Span Reciprocal Lattice Space	15
	Calculation of Potentials	16
	Truncation of Fourier Series	16
	Span K Space	17
	Calculation of KE Term and Feed Into Matrix	17
	Eigenvalues	17
	Wavefunctions	18
IV.	ENERGY BANDS	25
	Diffraction potential	25
	Vanishing Band Gaps in One Dimension	28
	Mathieu Potential	30
	Kronig-Penney Potential	32
	Triangular potential	37
	Exact solution for a single triangular well	37
	Comparison of the two methods	40
	Triangular potential with a plateau	44
	Superlattice potential	49
	Some Explanation of Zero Band Gaps	54
V.	WAVEFUNCTIONS	56
	Test Wavefunction	57
	Ψ^2 for Lowest Band of Mathieu Potential	62
	Ψ^2 for other Potentials Using (15x15) Plot	64

VI.	CONCLUSIONS	70
VII.	BIBLIOGRAPHY	73
	BIBLIOGRAPHY	74
VIII.	APPENDIX	77
	Triangular Potential	78
	Triangular Potential with Plateau	79
	Superlattice Potential	80

LIST OF FIGURES

<u>Figure</u>	<u>page</u>
4.1. Fourier series for various potentials	27
4.2. Energy vs. potential strength for Mathieu potential	31
4.3. KP potential with well width one fifth the period	32
4.4. Energy vs well depth for KP potential, $b = 1/5$ a	35
4.5. Energy vs well depth for KP potential, $b = a$	36
4.6. Energy vs. potential for Triangular potential	43
4.7. Well width equal to one fifth the period	44
4.8. Well width equal to one fifth the period	46
4.9. Well width equal to one half the the period	47
4.10. Plateau Vanishes	48
4.11. (AB) Superlattice	49
4.12. Superlattice potential, well 2 = $1/2$ size of well 1	51
4.13. Superlattice potential, well 2 = size of well 1	52
4.14. Superlattice potential, well 2 = five times size of well 1	53
5.1. Probability density of electrons subject to Mathieu Potential, $K=0$	60
5.2. Probability density of electrons subject to Mathieu Potential, $K=1$	61
5.3. Three dimensional plot of $ \psi ^2$	63

5.4.	Probability amplitudes of electrons subject to a Kronig-Penney potential	66
5.5.	Probability amplitudes of electrons subject to a Triangular Potential	67
5.6.	Probability amplitudes of electrons subject to a Triangular Potential with a Plateau	68
5.7.	Probability amplitudes of electrons subject to a Superlattice Potential	69

Chapter I

INTRODUCTION

Recent calculations of one-electron energy bands using the Plane Wave Diffraction (PWD) Method have been quite successful (Loly and Bahurmuz, 1979, 1980, 1981). The low-lying bands of the Mathieu and Kronig-Penney potentials have been described well by this method. This earlier interest concerns bands near or below the tops of the potential barriers, that is, bound, rather than ionized states.

Several other simple but important potentials are considered here. They include the one-dimensional triangular potential, a triangular potential with a plateau between the wells, and a superlattice potential.

The triangular potential is interesting for several reasons. First, it is simply characterized mathematically. Secondly, this potential can be made synthetically (Gossard et al, 1982). Thirdly, it has an interesting atomic limit which is quite distinct from the Kronig-Penney and Mathieu potentials. In fact, this one-dimensional power law potential is a confining potential, but is narrow at the bottom because of its decreasing width. The energy level spacing is expected to be different from other atomic wells, and this difference will also be seen in the periodic case.

since semiconductor lasers may be made from synthetic materials, it is important to establish their energy level separation pattern.

Fortunately, recent activity in connection with the spectra of power law potentials has provided numerical solutions and asymptotic formulae for the one-dimensional linear power potential (Ashbaugh and Morgan, 1981). The PWD results compare accurately with these atomic results, as well as showing the bandstructure of the corresponding periodic case.

The triangular well with a plateau between the wells is a logical extension of the pure triangular case, and has recently been examined by Lin and Smit (1981). Their primary motivation was the investigation of zero band gaps in the ionized region. The PWD Method, too, is used to investigate the bandstructure of this potential, demonstrating the existence of these zero gaps.

The superlattice potential, as well as the triangular type potentials, can be made synthetically by a process known as Molecular Beam Epitaxy. Traditionally, examples of electrons subject to various profiles have been restricted to naturally occurring systems (Kolbas, 1984). Now, by this process, these various potential profiles can be made synthetically. It is because these potentials are physically realizable, as well as mathematically simple, that they are of interest.

In this method, a layer of one material, such as gallium arsenide is placed between two layers of another material, such as aluminum gallium arsenide. This structure creates a potential well. If several sets of these layers are produced, a periodic system of potentials is formed. Various potential profiles have been made using this method. They include a parabolic quantum well (Miller et al, 1984) and the triangular potential (Gossard et al, 1982).

The energy bands of electrons subject to these potentials are calculated for both bound and ionized regions of the crystal lattice. The ionized regions exhibit vanishing gaps for certain potentials, a topic that has received renewed attention in the recent literature. Some physical criteria for these vanishing gaps are then discussed.

Finally, the electronic wavefunctions in the above crystals are studied. The probability density for electrons subject to such potentials are then computed.

Chapter II

SOME METHODS OF ONE-DIMENSIONAL BANDSTRUCTURE CALCULATIONS

One must make some assumptions before beginning any band-structure calculations. Two assumptions are made in the techniques reviewed here.

In the first assumption the crystal is regarded as a perfect periodic structure. Although this is an artificial representation of a real crystal, it is convenient mathematically, and does yield sensible results.

In the second simplifying assumption, the electron is assumed to move independently of all other electrons. Each electron is affected by the crystal potential and the average potential of all other electrons. This assumption is called the one-electron approximation.

Thus the task is to solve the one electron Schrodinger Wave Equation (SWE)
$$\left[-\frac{\hbar^2}{2m} \frac{d^2}{dx^2} + V(x) \right] \Psi(x) = E \Psi(x)$$

for the allowed energies and wavefunctions.

Early studies of this problem have been considered impractical because very few one-dimensional systems existed. Now, however, one-dimensional systems can be synthetically manufactured by Molecular Beam Epitaxy (MBE). Thus there has been a revival of interest in the solution of the SWE with a periodic potential. Several methods for its solution are presented here.

For a few potentials, the SWE can be solved exactly. These potentials include the Kronig-Penny potential (Kronig and Penney, 1931), the Mathieu potential (Pol and Strutt, 1928) and the potential $V(x) = -\text{csc}^2(\pi x/a)$ (Scarf, 1958). Another potential for which the Schrodinger Wave Equation can be solved completely is the potential $V(x) = (1-\gamma^2)(1-2\gamma \cos x + \gamma^2)$ where $0 \leq \gamma \leq 1$ (Wille et al, 1983). However, the number of potentials for which the SWE can be solved exactly is small, and numerical techniques must be used, in general.

Numerical integration is a direct technique of solving the SWE (Lin and Smit, 1981). A value of E , Ψ , and $d\Psi/dx$ is chosen at one point. Then the SWE is numerically integrated to yield $\Psi(x)$ at any other point. The value of k , the wavevector, must then be found after Ψ has been computed.

An alternative to numerical integration is the technique of transforming Schrodinger's differential equation into a difference equation. The resulting difference equation can

be solved by the method of continued fractions (Vigneron and Lambin, 1979). Basically, an energy value is chosen and substituted into a recurrence relation involving the energy and Bloch wavefunction. This recurrence relation is then solved using a continued fraction approach. After some algebra, an equation is provided for determining whether or not the chosen value of energy is indeed a solution of the SWE. It is a quick, efficient method, but one must have some idea of the energy before the calculation begins.

Alternately, a variational technique could be used to solve the SWE for the allowed energies and wavefunctions (Clarke and Martin, 1980). In this procedure, the unknown wavefunction is expressed in terms of a linear combination of basis functions. In symbols, the wavefunction would be written as $\Psi(x) = \sum_l c_l \chi_l$. This wavefunction is substituted into the expression for the energy expectation value,

$$\langle E \rangle = 1/N \int \Psi^*(x) H \Psi(x) dx.$$

When $\langle E \rangle$ is minimized with respect to the coefficients of the wavefunction expansion, a set of linear equations is obtained. These linear equations are solved for energies and wavefunctions.

Finally, the PWD method is another way of transforming the SWE into a set of algebraic equations, and solving them. This method is the subject of this study and is examined in detail in the next chapter.

Basically, the periodic potential of a crystal lattice is expanded in a Fourier series, and the electronic wavefunction is expanded in terms of plane waves. These expansions are substituted into the SWE, converting it to an algebraic equation. This method is conceptually simple, can be extended to two or three dimensions (Loly and Bahurmuz, 1979), and, as will be seen, yields good results.

Chapter III

PWD METHOD

The PWD method is used to calculate the bandstructures of electrons subject to simple potentials. The details of this method are presented here.

To begin the study of this method, we assume that there is a periodic chain of identical atoms, each having a given potential. By Bloch's Theorem the wavefunction of an electron in this periodic potential can be expanded in terms of plane waves:

$$\Psi(r) = \sum_G \alpha_{k-G} e^{i(\vec{k}-\vec{G}) \cdot \vec{r}} \quad (1)$$

Where k is the wavevector and G is a reciprocal lattice vector.

Usually, at the beginning of bandstructure problems, the spatial distribution of the potential energy must be determined, often by self-consistent methods (Koelling, 1981). Let's assume though that we know the potential beforehand. In this study, the potential would be one of the potentials mentioned in the introduction. Because this potential is periodic it can be expanded in a Fourier series

$$V(r) = \sum_G V_G e^{i\vec{G} \cdot \vec{r}} \quad (2)$$

For example, in one-dimension, we can write

$$\begin{aligned}
 V(x) &= \sum_n V_n e^{i(2\pi n/a)x} \\
 &= V_0 + 2V_1 \cos(2\pi x/a) + 2V_2 \cos(4\pi x/a) + \dots
 \end{aligned}$$

In the one-dimensional case $G_n = 2\pi n/a$, $n = 0, \pm 1, \pm 2, \dots$

Next, consider the one electron approximation where electrons move in the potential of the ion cores and the average potential of the other electrons. This potential is denoted by $V(r)$. The SWE then becomes :

$$(-\hbar^2/2m \nabla^2 + V(r)) \Psi_k(\vec{r}) = \epsilon(k) \Psi_k(\vec{r})$$

Substituting (1) and (2) into the SWE yields

$$\left[-\frac{\hbar^2}{2m} \nabla^2 + \sum_{G''} V_{G''} e^{i\vec{G}'' \cdot \vec{r}} \right] \sum_{G'} \alpha_{k-G'} e^{i(\vec{k}-\vec{G}') \cdot \vec{r}} = \epsilon(k) \sum_{G'} \alpha_{k-G'} e^{i(\vec{k}-\vec{G}') \cdot \vec{r}}$$

Operating and regrouping yields

$$\sum_{G'} \alpha_{k-G'} \left[\frac{\hbar^2(\vec{k}-\vec{G}')^2}{2m} - \epsilon(k) \right] e^{i(\vec{k}-\vec{G}') \cdot \vec{r}} + \sum_{G'} \sum_{G''} \alpha_{k-G'} V_{G''} e^{i(\vec{k}-\vec{G}'+\vec{G}'') \cdot \vec{r}} = 0$$

Denoting $\frac{\hbar^2(\vec{k}-\vec{G}')^2}{2m}$, the energy of the electron in the scattered state $k-G$, by $E_{k-G'}$ the expression can be written as

$$\sum_{G'} \alpha_{k-G'} [E_{k-G'} - \epsilon(k)] e^{i(\vec{k}-\vec{G}') \cdot \vec{r}} + \sum_{G'} \sum_{G''} \alpha_{k-G'} V_{G''} e^{i(\vec{k}-\vec{G}'+\vec{G}'') \cdot \vec{r}} = 0$$

By multiplying through by $e^{-i(\vec{k}-\vec{G}') \cdot \vec{r}}$ and integrating over all space, we obtain

$$\sum_{G'} \alpha_{k-G'} [E_{k-G'} - \epsilon(k)] \int_{\text{all space}} e^{i(\vec{k}-\vec{G}') \cdot \vec{r}} d\vec{r} + \sum_{G'} \sum_{G''} \alpha_{k-G'} V_{G''} \int_{\text{all space}} e^{i(\vec{k}-\vec{G}'+\vec{G}'') \cdot \vec{r}} d\vec{r} = 0$$

Noting that

$$\int_{\text{all space}} e^{i(\vec{a}-\vec{b}) \cdot \vec{r}} d\vec{r} = \delta_{ab}$$

one arrives at the infinite set of algebraic equations for the energy spectrum

$$\alpha_{k-G} (E_{k-G}^0 - E(k)) + \sum_{G'} \alpha_{k-G'} V_{G'-G} = 0 \quad (3)$$

This equation is equivalent to the original wave equation, but easier to work with.

These expressions express the fact that an electron in state k is scattered to state $k-G$ by the ionic potentials (Bahurmuz and Loly, 1981). E_k^0 is the free electron energy, whereas $E(k)$ is the energy of an electron in state k . We obtain non-trivial solutions of this equation by setting the determinant of coefficients equal to zero,

$$\det | (E(k) - E_{k-G}^0) \delta_{GG'} - V_{G-G'} | = 0 \quad (4)$$

If $G = G'$, the potential term becomes V_0 , a constant average potential. Thus the diagonal terms of the determinant represent the kinetic energy (KE) of the diffracted electrons to within the constant average potential.

If $G \neq G'$, the first term in the determinant, the kinetic energy term, vanishes, leaving only the potential term. Thus the off-diagonal terms of the determinant represent the Fourier coefficients of the periodic potential.

At this point, the analysis will be restricted to one dimensional problems, although the formalism so far applies to two and three dimensions as well.

In one-dimension the reciprocal lattice vectors become

$$G = 2\pi l/a \quad l = 0, \pm 1, \pm 2, \pm 3 \dots$$

as mentioned before. The potential becomes

$$V(x) = \sum_l V_l e^{i(2\pi l/a)x}$$

Since the potentials of the ion cores are real, $V_l = V_{-l}$. Some scale changes (Loly and Bahurmuz, 1981) are made to simplify the calculations.

Energies

The energies are referred to the bandwidth of the lowest free energy band,

$$E = \hbar^2 (\pi/a)^2 / 2m$$

$$\epsilon_k = E_k / E_0$$

Wavevectors

The wavevectors are normalized to the Brillouin Zone Wavevector, $k_{BZ} = (\pi/a)$

$$k = K (\pi/a)$$

$$K = k/k_{BZ}$$

yielding a first Brillouin Zone from -1 to +1.

Thus the determinant becomes

$$\det \left| (h^2(k-g)^2/2m - h^2k^2/2m) \delta_{gg'} - V_{g'-g} \right| = 0$$

Or, substituting the scale changes,

$$\det \left[(K - 2l)^2 - \epsilon_{ll} \right] \delta_{ll'} + V_{l'-l} = 0$$

And setting

$$t_l = (\hbar - 2l)^2 - E_k + V_0$$

$$v = v_l / E_0$$

the determinant becomes,

$$\begin{bmatrix} t_l & v_1 & v_2 & \dots & v_n \\ v_1 & & & & \cdot \\ \cdot & & t_0 & & \cdot \\ \cdot & & & & \cdot \\ v_n & & & & t_l \end{bmatrix}$$

But since $v_l = v_{-l}$, the determinant is symmetric

$$\begin{bmatrix} t_l & & & & \cdot \\ v_1 & t_{-l-1} & & & \cdot \\ & & t_0 & & \cdot \\ & & & & \cdot \\ v_l & & & & t_l \end{bmatrix} \quad (5)$$

The problem of solving

$$\det \left| (E_{\frac{D}{\hbar^2 - G}} - E(k))^2 + v_{\frac{G'-G}{G}} \right| = 0$$

is simplified to finding the eigenvalues and eigenvectors of the real symmetric matrix (5). The diagonal terms are the KE terms, and the off-diagonal terms are the Fourier coefficients of the potential energies.

The eigenvalues of this matrix are the reduced energies, E_k/E_0 , referred to the constant energy level V_0 . The eigenvectors are the coefficients of the wavefunctions, α .

The wavefunctions themselves can then be found by substituting these coefficients into expression (1).

Thus, the Fourier series for a given potential is the input, and the energies and wavefunctions are the output.

3.1 COMPUTER CODING OF PROBLEM

Next, the numerical procedure is outlined.

We want to find the eigenvalues and eigenvectors of the real symmetric matrix

$$\begin{bmatrix} t_{-l} & & & & \\ v_l t_{-l-1} & & & & \\ & t_0 & & & \\ & & & & \\ v_l & & & & t_l \end{bmatrix}$$

The program computes the values of t_l and v_l , and then feeds these values into the matrix. The eigenvalues and eigenvectors are then found using the IMSL subroutine EIGRS. The major segments of the program consist of:

1. Initialization
2. Spanning Reciprocal Lattice Space
3. Calculate Potentials and Feed Them into Matrix
4. Truncation of Fourier Series

5. Span K Space
6. Calculate KE terms and Feed them into Matrix
7. Find Energy Eigenvalues
8. Find Wavefunctions

The program is coded in Fortran.

3.1.1 Initialization

This section specifies such things as variable type and dimensions.

A(NSYM) is the input real symmetric matrix, stored in half storage mode. It has dimension $NSYM = NRECIP(NRECIP+1)/2$, where NRECIP is the number of reciprocal lattice vectors.

M(NSYM) is the matrix which feeds the values of t and v into the matrix A.

D(NRECIP) is the output vector containing the eigenvalues.

Z is the output (NRECIP*NRECIP) matrix containing the eigenvectors of matrix A. Eigenvectors in column J of Z correspond to eigenvalues D(J).

WK(NRECIP) is the 'work area' used by EIGRS.

V(NRECIP) is the vector containing the values of the potential energy.

B(_) is the vector containing the amplitude of the potential. Its dimension is the number of different amplitudes one wishes to investigate.

YY(K,L) is the matrix containing the energy eigenvalue, L , for a given wavevector, K . The dimension of K is the number of wavevectors one is interested in, and the dimension of L is at most NRECIP.

G(NRECIP) is the reciprocal lattice vector.

NVEE is the number of potentials one wishes to examine.

NK is the number of wavevectors one wishes to use.

QSO is the effective mass of the electron. It is set to 1 for all the following calculations.

PURPSE This program can calculate energies and/or wavefunctions. If purpse=1, it calculates energies only. If purpse=2, it calculates wavefunctions only. If purpse=3, it calculates both energies and wavefunctions.

3.1.2 Span Reciprocal Lattice Space

Both the potential and the wavefunctions are summed over the reciprocal lattice vector, G . The number of reciprocal lattice vectors can be varied in the program.

In the notation of the program, NSTAR determines the number of reciprocal lattice vectors to be used. For example,

NSTAR = 1 $G = 0, \pm 2\pi/a$

NSTAR = 2 $G = 0, \pm 2\pi/a, \pm 4\pi/a$

NNNEYB = number of shells of neighbors = 2(NSTAR)

NRECIP = 2(NNNEYB) + 1 = number of reciprocal lattice vectors

3.1.3 Calculation of Potentials

To calculate the Fourier coefficients of the potential, a subroutine, POTEN which calculates the potentials, is invoked.

POTEN(V,AV,B)

V = Fourier Coefficients

AV = V term, or the $G = G$ term

B = Amplitude of the potential, or the strength of diffracting potentials

These coefficients are fed into the off-diagonal elements of the matrix.

3.1.4 Truncation of Fourier Series

In theory, the summation of the Fourier series over the index, n , which is related to the reciprocal lattice vector, is infinite. However, most of the potentials studied here have Fourier coefficients which are proportional to $1/n$ or $1/n^2$, and can be truncated. Fifteen terms is more than adequate to truncate the series. The higher coefficients of the Fourier series contribute very little to the overall sum.

3.1.5 Span K Space

Recall that an electron is being scattered from state k to state $k-G$. The energies and wavefunctions, naturally, depend upon the electronic state, k .

The program calculates the energy eigenvalues for these electrons for any number of wavevectors, k .

The program uses the reduced variable $RKVECT$, which ensures a k -vector between the zone centre, $K=0$, and the zone boundary, $k=1$. In the program, $RKVECT = (k-1)/(NK-1)$ where $0 \leq (k-1) \leq (NK-1)$, so $0 \leq RKVECT \leq 1$.

3.1.6 Calculation of KE Term and Feed Into Matrix

The KE term is

$$t_k = (K - 21)^2 + E_k + V_0$$

In the terminology of the program,

$$A = KVECT - 2(I-NSTAR-1)^2/QSQ + AV$$

Recall that QSQ , the effective mass, is set to one.

3.1.7 Eigenvalues

The energy eigenvalues are then calculated by the EIGRS subroutine (IMSL).

3.1.8 Wavefunctions

The expression for the wavefunction, as mentioned earlier, is

$$\Psi_k(x) = \sum_k \alpha_{k-G} e^{i(k-G)x}$$

where α_{k-G} is the coefficient of the plane wave $e^{i(k-G)x}$.

Computationally, it is quite easy to obtain the coefficients α . They are the eigenvectors of the programmed determinant, normalized to one.

This eigenvector, labelled Z in the program, is then multiplied by the plane wave $e^{i(k-G)x}$, and summed over all k.

$|\Psi|^2$, the probability density of the electrons, is then easily found.

Computer Program

```

C   DIFFRACTION MODELLING OF ELECTRON BAND STRUCTURES
C   THIS PROGRAM CALCULATES THE ENERGIES AND WAVEFUNCTIONS
C   IN A ONE ELECTRON APPROXIMATION, OF ELECTRONS IN A
C   SOLID, SUBJECT TO A GIVEN IONIC POTENTIAL
C   TO CALCULATE:
C       A) ENERGIES ONLY, SET PURPSE = 1
C       B) WAVEFUNCTIONS ONLY, SET PURPSE = 2
C       C) ENERGIES AND WAVEFUNCTIONS, SET PURPSE = 3

```

```

C   SPECIFICATION STATEMENTS

```

```

IMPLICIT REAL*8(A-H,O-Z)
COMPLEX*16  PWAVE,EYE,WF1,WF2,WF3,TOTWF1,TOTWF2,TOTWF3
DIMENSION M(15),A(120),D(15),Z(15,15),WK(15),V(15),B(20)
DIMENSION YY(2,4),G(15)
DATA NVEE,NK,QSQ /20,2,1.0D0/
COMMON NNNEYB,IC,NRECIP
EYE=DCMPLX(0.0D0,1.0D0)
PURPSE=1

```

```

C
DO 100 NSTAR=7,7
NNNEYB=2*NSTAR
NRECIP=NNNEYB+1
IZ=NRECIP
MDPT=(NRECIP+1)/2

```

```

C
C   SET UP POTENTIALS

```

C

```
DO 901 IC=1,NVEE
CALL POTEN(V,AV,B)
```

C

C

C

TRUNCATION OF FOURIER SERIES

C

```
DO 700 NV=1,1
```

C

```
NN=NRECIP+1-NV
```

```
WRITE (6,353) NN
```

```
353 FORMAT (1X,'NO. OF TERMS REPRESENTING THE POTENTIAL IS',I3)
```

```
DO 701 I=NN,NRECIP
```

```
V(I)=0.0D0
```

```
701 CONTINUE
```

C

C-----

C

DIAGONAL INDICES

C

```
M(1)=1
```

```
DO 1 I=2,NRECIP
```

```
M(I)=M(I-1)+I
```

```
1 CONTINUE
```

C

C-----

C

SPAN K-SPACE

C

```
DO 5 K=1,NK
```

C

$$RKVECT = (DFLOAT(K-1)) / DFLOAT(NK-1)$$

C-----

C

C OFF DIAGONAL ELEMENTS

C

DO 2 I=2,NRECIP

INT=I-1

DO 3 J=1,INT

$$A(M(INT)+J) = V(I-J)$$

3 CONTINUE

2 CONTINUE

C

C-----

C DIAGONAL ELEMENTS

C

DO 6 I=1,NRECIP

$$A(M(I)) = (RKVECT - DFLOAT(2*(I-NSTAR-1))) ** 2 / QSQ + AV$$

6 CONTINUE

C

C-----

C

FIND EIGENVALUES

C

IF (PURPSE.NE.1) GO TO 279

CALL EIGRS(A,NRECIP,0,D,Z,IZ,WK,IER)

GO TO 291

279 CALL EIGRS(A,NRECIP,1,D,Z,IZ,WK,IER)

IF (PURPSE.EQ.2) GO TO 294

C

C

STORE EIGENVALUE DATA

C

291 CONTINUE

DO 8 L=1,4

YY(K,L)=D(L)

8 CONTINUE

C-----

C

C

WRITE EIGENVALUES

C

WRITE (6,510)

WRITE (6,499) RKVECT

499 FORMAT (' K=',F3.1)

WRITE (6,510)

WRITE (6,522)

522 FORMAT(1X,'ENERGY EIGENVALUES')

WRITE (6,510)

WRITE (6,500) D

500 FORMAT (10E13.5)

WRITE (6,510)

510 FORMAT (' ')

WRITE(6,510)

5 CONTINUE

C

C

STORE AMPLITUDE AND EIGENVALUES ON DATA FILE

C

WRITE(8,205) B(IC),YY(1,1),YY(2,1),YY(1,2),YY(2,2),

```
      $YY(1,3),YY(2,3),YY(1,4),YY(2,4)
205  FORMAT(F6.2,2X,8(E13.5,2X))
C
      IF (PURPSE.EQ.1) GO TO 613
C      WRITE EIGENVECTORS
C
C      FIND WAVEFUNCTIONS
C
294  WRITE(6,296)
296  FORMAT(3X,'X',8X,'PROB1',8X,'PROB2',11X,'PROB3')
      DO 512 IX=1,61
          X=0.1D0*DFLOAT(IX-31)
          TOTWF1=DCMPLX(0.0D0,0.0D0)
          TOTWF2=DCMPLX(0.0D0,0.0D0)
          TOTWF3=DCMPLX(0.0D0,0.0D0)
          DO 310 JJX=1,NRECIP
              G(JJX)=DFLOAT(MDPT-JJX)
              PWAVE=CDEXP(EYE*(RKVECT-G(JJX))*X)
              WF1=Z(JJX,1)*PWAVE
              WF2=Z(JJX,2)*PWAVE
              WF3=Z(JJX,3)*PWAVE
              TOTWF1=TOTWF1+WF1
              TOTWF2=TOTWF2+WF2
              TOTWF3=TOTWF3+WF3
310  CONTINUE
          PROB1=TOTWF1*DCONJG(TOTWF1)
          PROB2=TOTWF2*DCONJG(TOTWF2)
          PROB3=TOTWF3*DCONJG(TOTWF3)
```

```
WRITE(6,315) X,PROB1,PROB2,PROB3
WRITE(9,315) X,PROB1,PROB2,PROB3
315   FORMAT(F6.2,2X,E10.3,2X,E10.3,2X,E10.3)
512   CONTINUE
      NM=NN-1
      WRITE (6,520)
520   FORMAT (' ')
613   CONTINUE
700   CONTINUE
901   CONTINUE
100   CONTINUE
      STOP
      END
```


IV

ENERGY BANDS

When the determinantal equation (4) is solved, the solutions for E will fall into bands and gaps. The states within each allowed band will be labelled by k .

Actually, there are several ways energy bands can be presented (Bube, 1981). The energy could be plotted as a function of wavevector, k , expressing the dispersion relation for the electron wave. The energy could also be plotted as a function of crystal position, emphasizing the nonlocalized nature of bands. Alternately, one could plot energy as a function of the diffraction potential, a presentation which shall be adopted in this study. Finally, it should be mentioned that one could plot equal energy surfaces as a function of wavevector.

4.1 DIFFRACTION POTENTIAL

In order to use this PWD method, a potential must be chosen, and Fourier-analyzed as in equation (2).

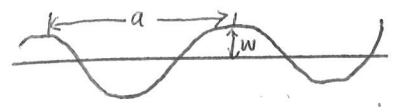
The question of the choice of potential may arise. Are they chosen for mathematical convenience, or do they model real, physical systems (Lieb and Mattis, 1965), or both? In the PWD Method, one can choose a real periodic potential.

It is interesting to note that the condition $V_l = V_{-l}$, ensuring a real potential, restricts this potential to an even function, $V(x)=V(-x)$. An even function, of course, is the only function where the Fourier coefficients V_l can equal the Fourier coefficients V_{-l} .

In this study, the band structure of electrons subject to five such potentials will be discussed. The first two potentials were chosen for comparison of the PWD with other methods of band structure calculations. The second three were chosen for their physical significance, as mentioned earlier.

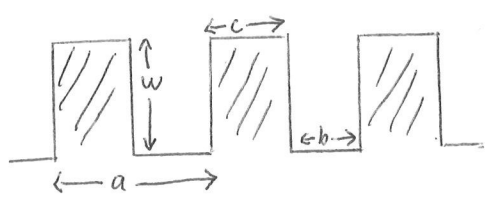
The Fourier series are presented in figure 4.1 and their derivation in appendix 1. The electron energies are then computed using these series and plotted as a function of potential well depth. All calculations use fifteen reciprocal lattice vectors of equation (3). A discussion of the features of the band structure will follow these calculations.

① MATHIEU POTENTIAL



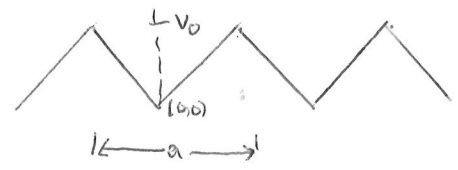
$$V(x) = 2W \left[1 - \cos\left(\frac{2\pi}{a}x\right) \right]$$

② KRONIG-PENNEY POTENTIAL



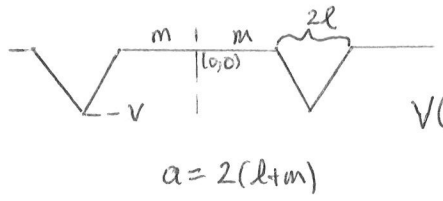
$$V(x) = \sum_n \left[\left(-\frac{W}{n\pi}\right) \sin\left(\frac{n\pi c}{a}\right) \right] \cos\left(\frac{2n\pi}{a}x\right)$$

③ TRIANGULAR POTENTIAL



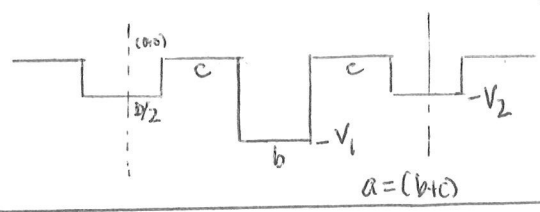
$$V(x) = \frac{V_0}{2} + \frac{4V_0}{\pi^2} \sum_{n=1}^{\infty} \frac{1}{n^2} \left[(-1)^n - 1 \right] \cos\left(\frac{2n\pi}{a}x\right)$$

④ TRIANGULAR POTENTIAL WITH PLATEAU



$$V(x) = \frac{-Vl}{2(l+im)} + \sum_{n=1}^{\infty} \frac{2V(l+im)}{l(n\pi)^2} \left[(-1)^{n+1} + \cos\left[n\pi\left(\frac{m}{l+im}\right)\right] \right] \cos\left(\frac{2n\pi}{a}x\right)$$

⑤ (AB)_N SUPERLATTICE



$$V(x) = \frac{-b}{2(bc)} (V_2 + V_1) + \sum_{n=1}^{\infty} \frac{1}{n\pi} \left\{ -V_2 \sin\left(\frac{n\pi b}{2a}\right) - V_1 \sin\left(\frac{n\pi\left(\frac{3b}{2}+c\right)}{a}\right) + V_1 \sin\left(\frac{n\pi\left(\frac{b}{2}+c\right)}{a}\right) + V_2 \sin\left(\frac{n\pi\left(\frac{3b}{2}+2c\right)}{a}\right) \right\} \cdot \cos\left(\frac{2n\pi}{a}x\right)$$

Figure 4.1: Fourier series for various potentials

4.2 VANISHING BAND GAPS IN ONE DIMENSION

One usually thinks of an electron band structure diagram as consisting of distinct bands separated by gaps. However, for certain potentials these bands might touch at several points (Allen, 1953 or Lippmann, 1957).

The points where these bands touch are called points of contact (Allen, 1953) or simply, vanishing gaps. Two questions that naturally arise are when and why do these zero gaps occur ?

We shall examine some conditions where bandgaps disappear at certain potentials (Lin and Smit, 1981 or Strandberg, 1982). The potentials, it seems, must be confining, localized,¹ and symmetrical. Also, it seems (Lin and Smit, 1981) there must be a flat, intersitial region between wells, similar to the muffin tin method of band structure calculations (Ziman, 1971). Furthermore, vanishing gaps can only occur above the top of the barriers (Lippmann, 1957).

In previous studies (Loly and Bahurmuz, 1979,1980,1981) these zero band gaps were not encountered because those studies were concerned with low lying-bands and Kronig-Penney potentials with fixed depth.

¹ The word 'localized' is used loosely here, and this point is discussed in Chapter 6.

Incidentally, if one slightly varies the potential, the zero band gaps disappear. Thus they are sometimes referred to as vanishingly improbable phenomena (Herring, 1937).

4.3 MATHIEU POTENTIAL

The band structure of an electron subject to the Mathieu potential has already been examined using the PWD Method (Pincerle, 1961 and Loly and Bahurmuz, 1979). It is included in this study, though, to see if zero band gaps appear, and also because the wavefunction of an electron subject to this potential is examined later.

This potential has a well for the atomic cores and a hump for the interstitial region. It does not have a localized well, nor does it have a flat interstitial region. Hence it is not likely to have zero gaps.

The numerical evidence presented in figure 4.2 shows that there are no zero gaps for the Mathieu potential.

The allowed energy bands are plotted for the potential wells with variable well depth. The bottom of each band corresponds to the electronic energy for $k=0$, whereas the top of each band corresponds to the energy for $k=1$. For the Mathieu potential the bands are labelled B1 for the lowest band, B2 for the second band, B3 for the third band and B4 for the fourth band.

The energy band diagrams for the other potentials follow a similar pattern.

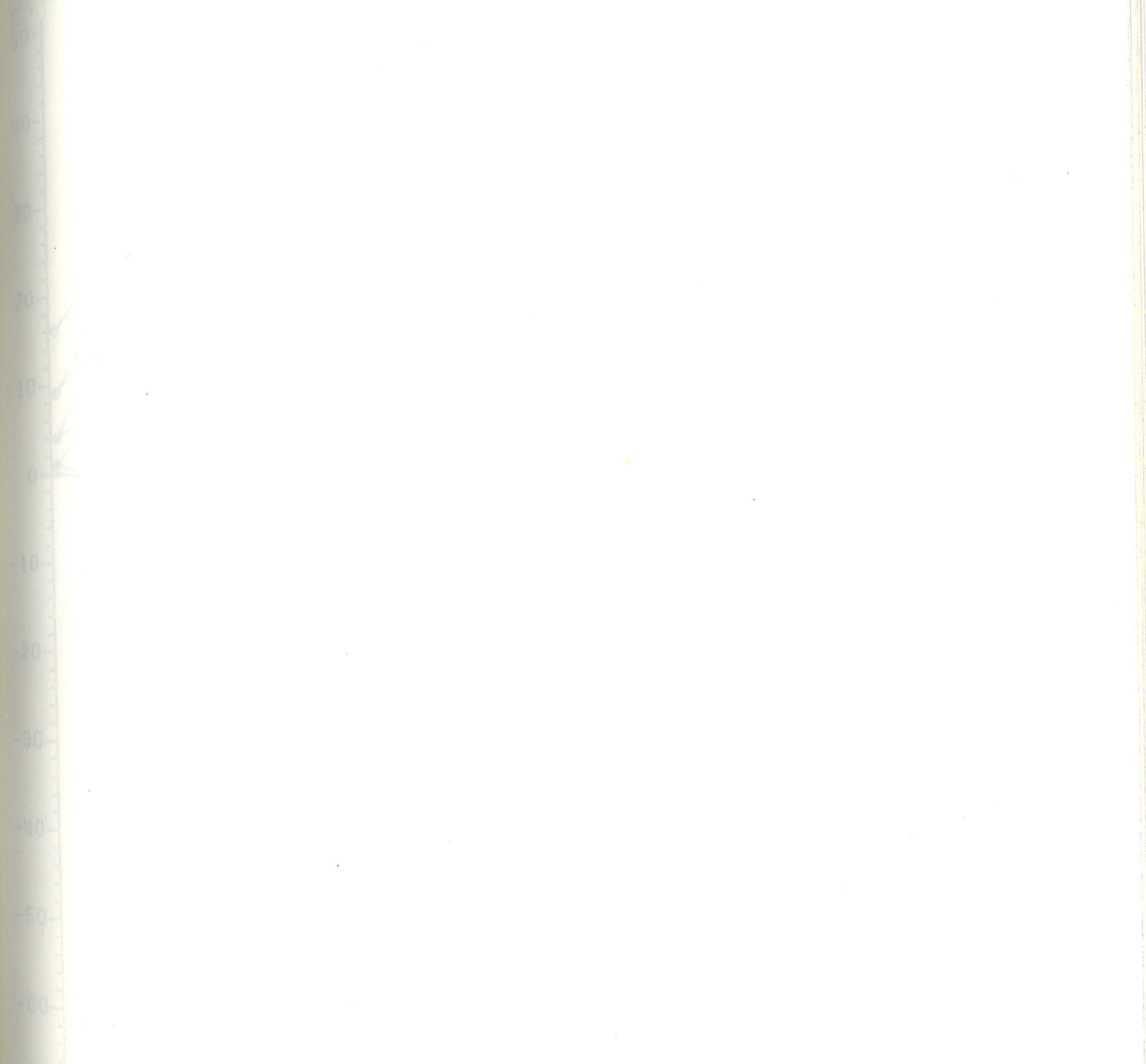
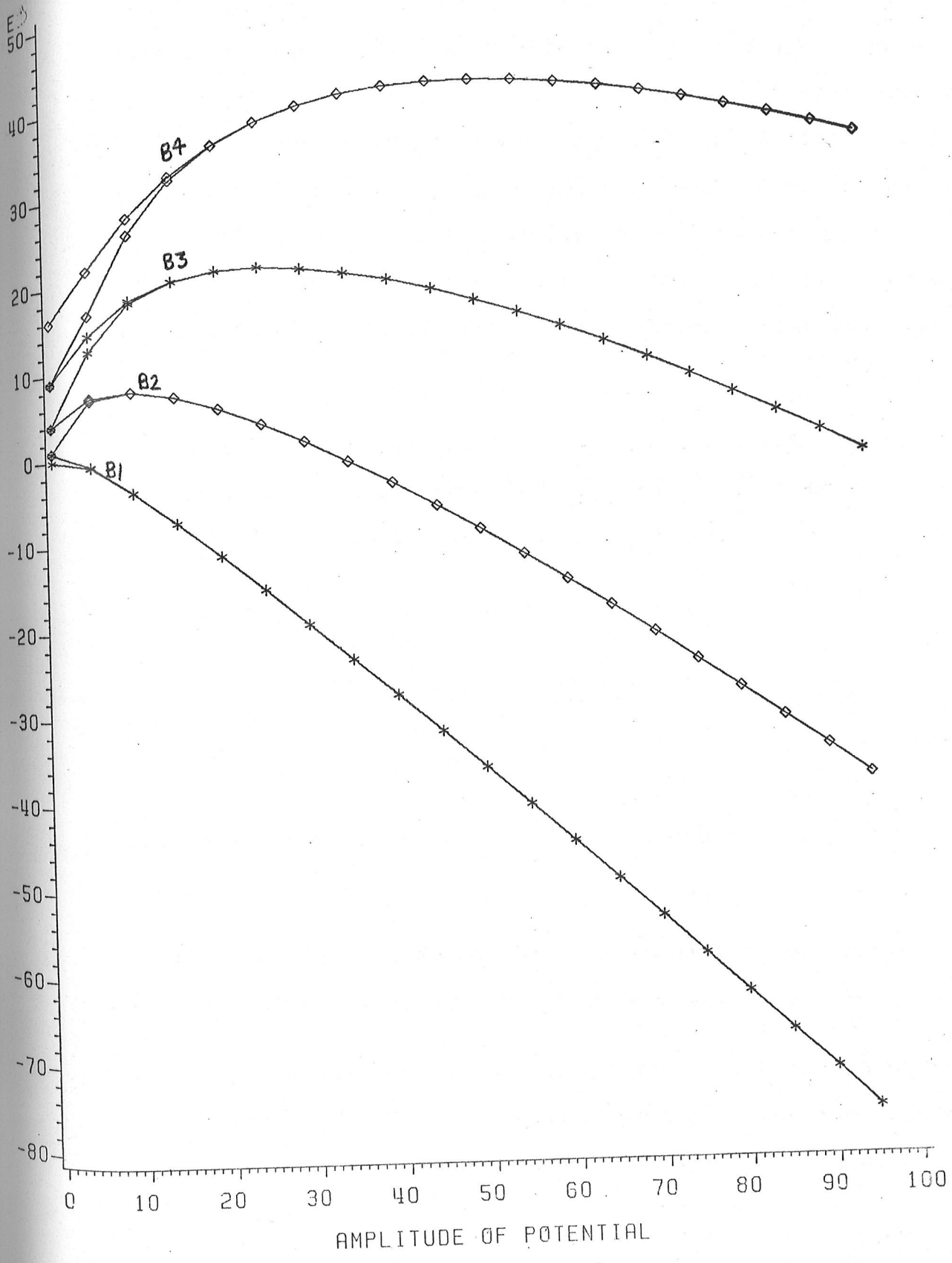


Figure 4.2: Energy vs. potential strength for Mathieu potential



4.4 KRONIG-PENNEY POTENTIAL

The energy band structure of the Kronig-Penney potential has been investigated with many methods (for example, see Wetzel, 1980), including the PWD Method (Loly and Bahurmuz, 1979). These workers were mainly interested in low-lying bands and did not study in detail the bands above the barrier. This problem is re-examined here, to see if the PWD method can reproduce the touching band gaps of previous studies (Lin and Smit, 1980), which appear above the barrier.

First, if the well width is set to one fifth the period, vanishing band gaps occur for 0, the free electron case, 19, 23.2, 98, as in figure 4.3,

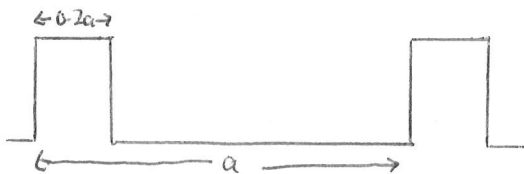


Figure 4.3: KP potential with well width one fifth the period

This configuration does have a localized well and a flat interstitial region, so vanishing band gaps are likely.

These results seem to be in agreement with the results of Lin and Smit (1980). They use a simple scattering argument to predict the location of zero band gaps. This argument is

presented in section 4.8, and the result is quoted below. They predict that for vanishing gaps, the well must have a depth of

$$V_0 = \left(\frac{\hbar^2 \pi^2}{2m} \right) \left(\frac{n_1^2}{b^2} - \frac{n_2^2}{c^2} \right)$$

where b is the width of the well, c is the width of the interstitial region, $a = (b+c)$ is the period, and n_1 and n_2 are integers.

Recalling that our potentials are divided by the factor $\left(\frac{\hbar^2 \pi^2}{2m} \right)$ we should expect gaps to occur at potentials

$$V_0 \sim \left(\frac{n_1^2}{b^2} - \frac{n_2^2}{c^2} \right)$$

Now $b=0.2a$ and $c=0.8a$, since the well width is one fifth the period.

Setting $n_1 = 0$ $n_2 = 0$ yields a gap at 0.00.

Setting $n_1 = 2$ $n_2 = 1$ yields a gap at 18.27.

Setting $n_1 = 1$ $n_2 = 1$ yields a gap at 23.4.

Setting $n_1 = 1$ $n_2 = 2$ yields a gap at 98.0. The results are presented in figure 4.4.

Now if the width of the well equals the length of the interstitial region, the band gaps vanish, as can be seen from figure 4.5.

The Kronig-Penney potential, too, seems to follow the conditions for vanishing band gaps. The well must be localized with a flat region in between. The zero gap energies, too, are greater than the diffracting potentials.

The Kronig-Penney potential is often used in textbooks and undergraduate lectures to illustrate the existence of bands and gaps. However, it is presented without localized wells, or approximated by delta function potentials, where zero gaps cannot occur (Allen, 1953).

50
40
30
20
10
0
-10
-20
-30
-40
-50
-60
-70
-80

Figure 4.4: Energy vs well depth for KP potential, $b = 1/5$
a The dashed line indicates the top of the well. The ionized region lies above this line, the bound region below.

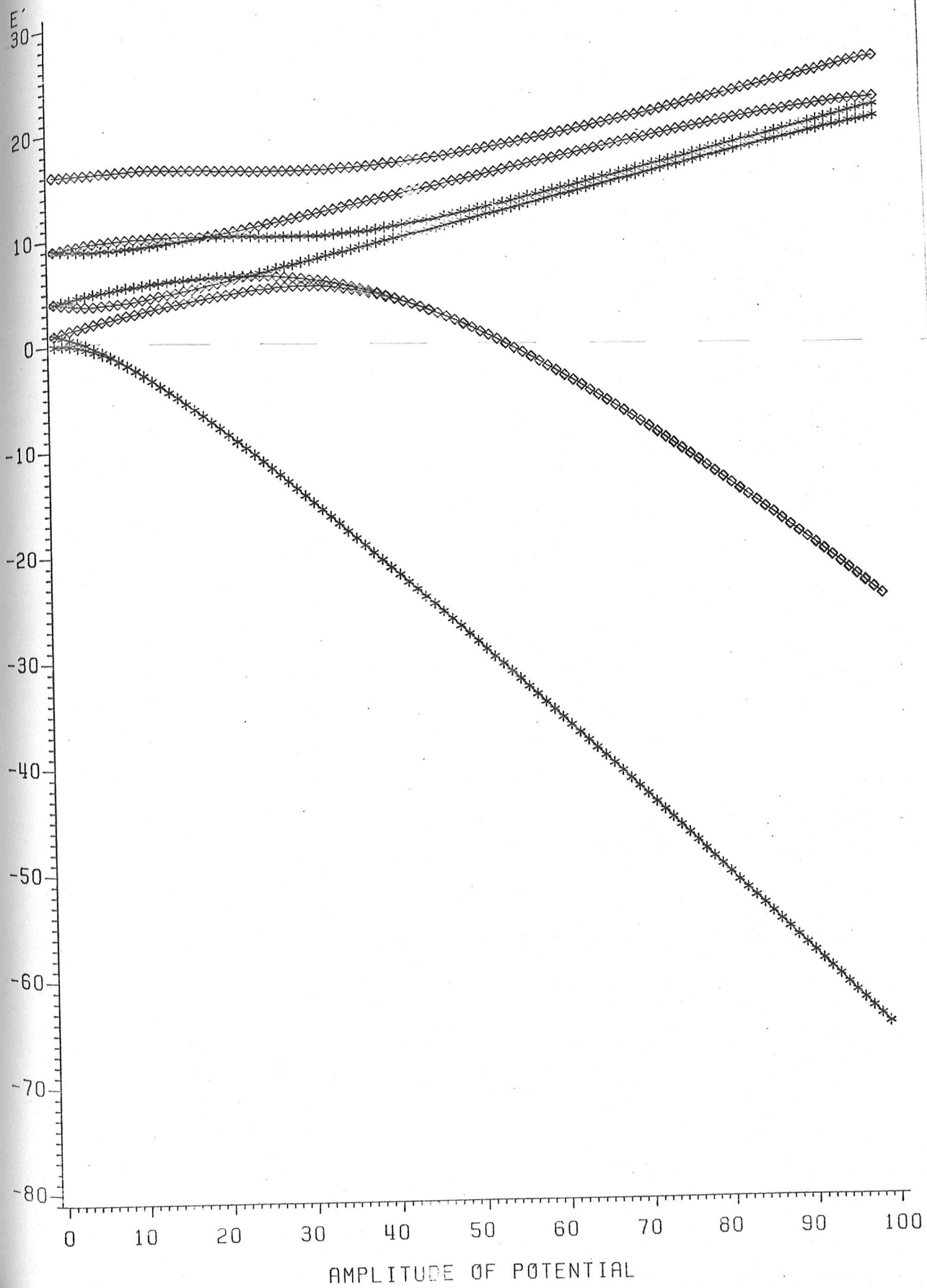
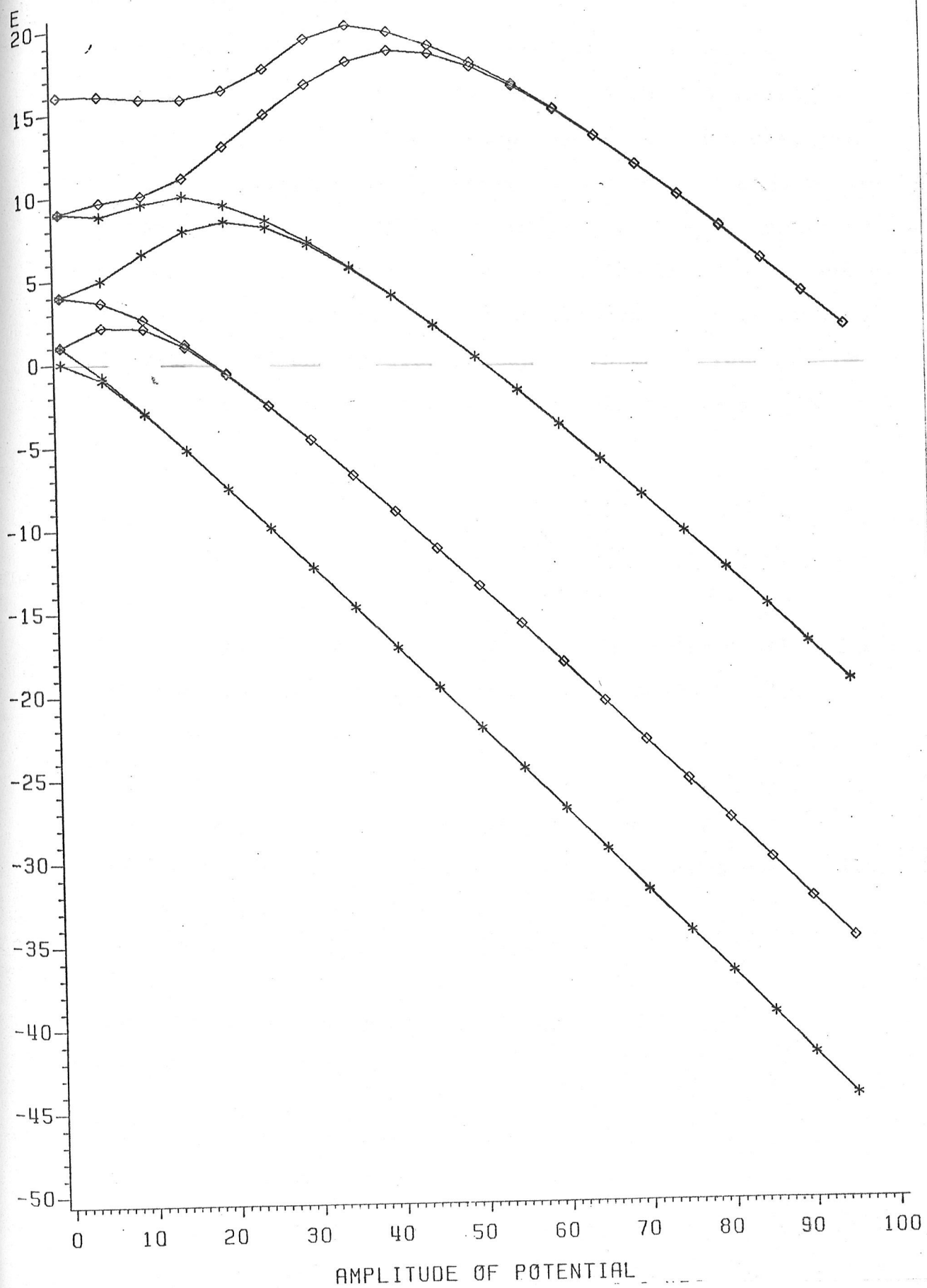


Figure 4.5: Energy vs well depth for KP
potential, $b = a$



4.5 TRIANGULAR POTENTIAL

First, the energy bands for an electron in a periodic triangular potential well are computed using the PWD method (Loly and Bahurmuz, 1979). These eigenvalues are then compared to the exact solution to the atomic or single triangular well problem (Ashbaugh and Morgan, 1981). For the PWD solution a series of electron bands, representing bound and unbound states can be computed, whereas the exact solution yields discrete bound energy eigenvalues. In the triangular periodic well problem of period 2π , the Fourier series is given by:

$$\frac{1}{A} f(x) = \begin{cases} 1 + \frac{x}{\pi} & -\pi \leq x \leq 0 \\ 1 - \frac{x}{\pi} & 0 \leq x \leq \pi \end{cases}$$

Thus the well has a slope of $A/\pi/2$. The slope of the single well used by Ashbaugh and Morgan corresponds to $2A/\pi = 1$ or $A = \pi/2$.

4.5.1 Exact solution for a single triangular well

The exact solutions for the energy eigenvalues are obtained from the SWE:

$$\frac{d^2\psi}{dx^2} + (E - c|x|)\psi = 0 \quad (AM)$$

for $x \geq 0$ and boundary conditions (b.c.) $\psi(\infty) = 0$

$\psi'(0) = 0$ even solution

$\psi(0) = 0$ odd solution and setting

$$x' = c^{1/3}(-E/c + x)$$

$$dx' = c^{2/3} dx^2$$

one arrives at Airy's differential equation

$$-\frac{d^2\psi}{dx'^2} + x'\psi = 0$$

Solving this equation with the above b.c. yields energies which are the solution to the zeroes of the Airy Function and its derivative

$$\text{Ai}(-Ec^{-2/3}) = 0$$

$\text{Ai}'(-Ec^{-2/3}) = 0$ where c is the amplitude of the potential.

The numerical results (i.e. the zeroes of the Airy Function) are taken directly from Ashbaugh and Morgan (1981). One must note however, that Ashbaugh and Morgan (1981) solve equation (AM) for $c=1$. The eigenvalues can easily be obtained for other values of c by the transformation used above. That is, if E is the eigenvalue for $c=1$, the energy for arbitrary c , is given by

$$E_c = E c^{2/3}$$

It is interesting also to note the expansion of the exact solution to Airy's differential equation. As given in Ashbaugh and Morgan:

$$E_n = \left[\frac{3}{4}\pi(n+\frac{1}{2}) \right]^{2/3} \left\{ 1 - \frac{7}{48} \left[\frac{3}{4}\pi(n+\frac{1}{2}) \right]^{-2} + O[(n+\frac{1}{2})^{-4}] \right\} \quad n \text{ even}$$

$$E_n = \left[\frac{3}{4}\pi(n+\frac{1}{2}) \right]^{2/3} \left\{ 1 + \frac{5}{48} \left[\frac{3}{4}\pi(n+\frac{1}{2}) \right]^{-2} + O[(n+\frac{1}{2})^{-4}] \right\} \quad n \text{ odd}$$

The common leading term is $3/4(n+1/2)^{2/3}$.

Thus we expect $E \sim (n+1/2)^{2/3}$, an interesting power law.

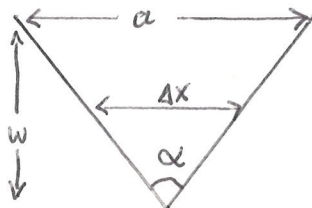
It is interesting to compare the dependence of energy on n , the principal quantum number, with the Mathieu and Kronig-Penney Potentials (Loly and Bahurmuz, 1980). The Kronig-Penney case resembles a square well, with $E \sim n^2$ whereas in the Mathieu case the bottom of the well is parabolic, and hence $E \sim (n+1/2)$ for deep wells.

The two thirds power law for the energy dependence on potential depth in equation (AM) is easily obtained by a simple quantum mechanical calculation using the Uncertainty Principle.

To see this, confinement is measured

by the "angle"

$$\alpha = \frac{a}{W}$$



where a = lattice parameter

W = depth of potential

The Uncertainty Principle is used

$$\Delta x \Delta p_x \geq \hbar$$

and energies are computed approximately from the kinetic formula

$$E = \frac{p^2}{2m}$$

For Δx one has $\Delta x = \alpha E_1$

for

$$\Delta p_x \sim \hbar / \alpha E_1$$

so that

$$E_1 \sim \left(\frac{\hbar}{\alpha E_1} \right)^2 / 2m = \frac{\hbar^2}{2m} \frac{1}{\alpha^2 E_1^2}$$

and finally

$$E_1^3 \sim \alpha^{-2}$$

for

$$E_1 \sim \left(\frac{\hbar^2}{2m} \right)^{1/3} \left(\frac{W}{a} \right)^{2/3}$$

4.5.2 Comparison of the two methods

Returning to the main problem, one can now compare some numerical results for bound eigenstates, derived from both the PWD approximation and the exact results for a single V shaped well.

AMPLITUDE FACTOR	SINGLE WELL	PERIODIC TRIANGULAR
C=1	1.0188	0.7352 to 1.0466
	4.7288	4.7075 to 4.7476
	10.8525	11.2049 to 10.4663
	15.0768	13.9122 to 16.8019
C=100	21.942	21.949 to 21.949
	50.3730	50.373 to 50.373
	69.9803	69.980 to 69.981
	88.0722	88.075 to 88.070

	103.8459	103.82 to 103.87
	118.9368	119.12 to 118.71
	132.7844	131.78 to 133.59
	146.2152	148.81 to 143.48
	158.8287	154.70 to 165.02
C=1000	101.8793	101.96 to 101.97
	233.8106	233.85 to 233.86
	324.8197	324.93 to 324.93
	408.7948	408.91 to 408.92
	1534.0751	1548.8 to 1571.4

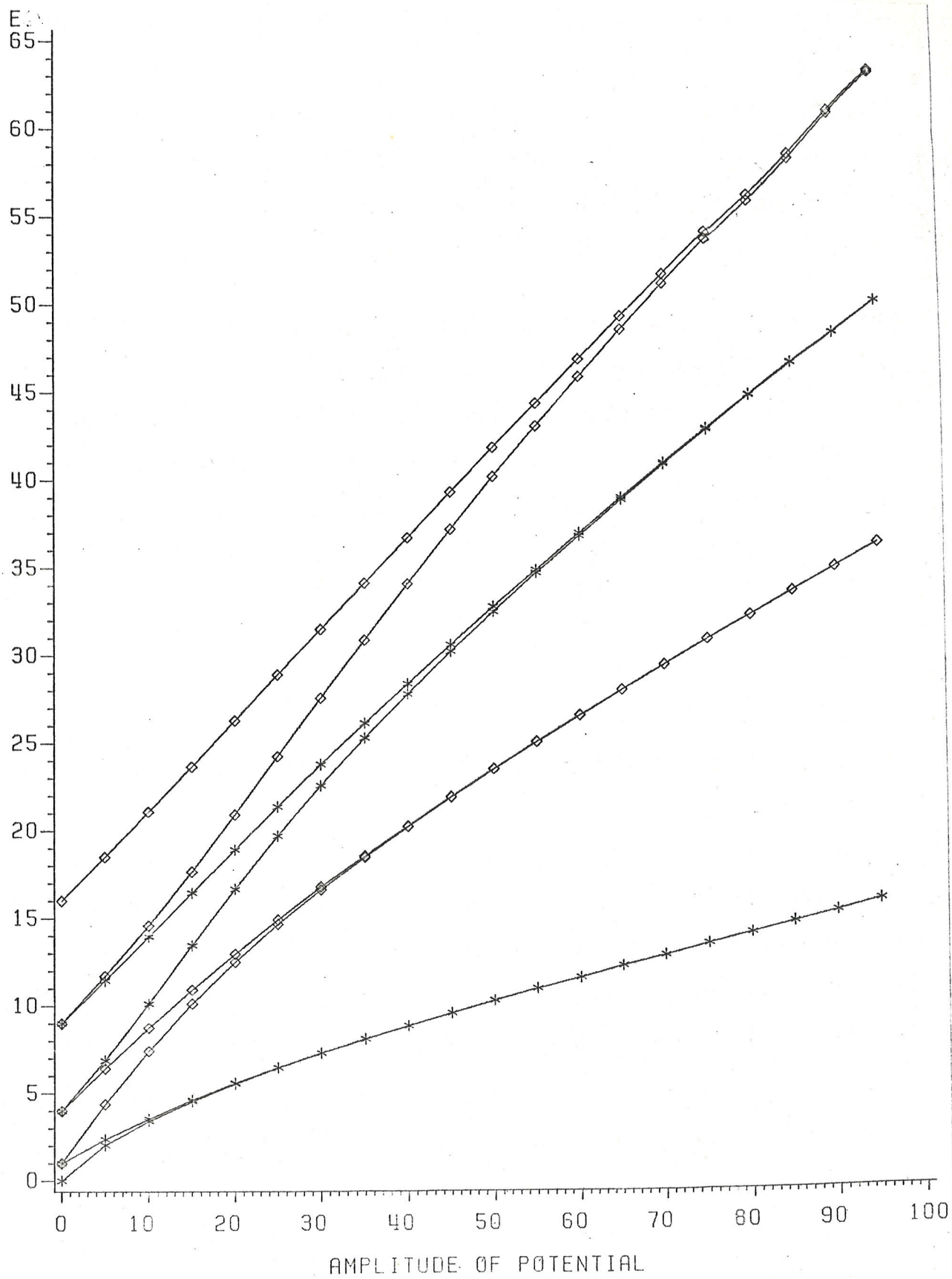
For potential barriers up to $c=100$, the exact bound state eigenvalues fall within the energy bands calculated by the PWD method. As c increases, however, to $c=1000$ and higher, the exact eigenvalues tend to lie a bit below the calculated energy bands. This disagreement probably indicates that a larger determinant is needed for complete agreement.

Even with this slight discrepancy for wells with large potentials the PWD method does indeed yield the eigenvalues of an electron in a triangular well potential.



Now we examine the overall band structure, as presented in figure 4.6. It consists of distinct bands which narrow with increasing potential. There are no vanishing band gaps, except, of course, for zero potential, the free electron case. It should be noted that the triangular potential has a well on the atomic cores, but no flat interstitial region. Hence, the energy spectrum of an electron subject to this potential does not have vanishing band gaps. One would predict this from the conditions for zero band gaps, as outlined earlier.

Figure 4.6: Energy vs. potential for Triangular potential



4.6 TRIANGULAR POTENTIAL WITH A PLATEAU

Next, a calculation of the energy band structure of a periodic triangular well with a plateau is examined. This problem has already been studied by another method (Lin and Smit, 1981), with interesting results. They found several vanishing band gaps, or "touching gaps" in the energy band structure.

Lin and Smit consider a well whose width is one fifth the period. So let's also consider the case of a localized triangular well, with the well width one fifth the period, as in figure 4.7.

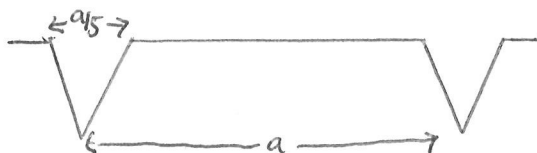


Figure 4.7: Well width equal to one fifth the period

It's band structure is presented in figure 4.8, with vanishing band gaps as one would guess, and as Lin and Smit have shown. Although the PWD energies are slightly higher than those presented by Lin and Smit (1981), the overall band structure diagram exhibits the same qualitative features, in particular, the zero band gaps.

Now if we widen the well, so the width is one half the period, we can observe that the previous band gaps disappear, because now the well is less localized.

Finally, if the plateau disappears altogether, the potential is just the triangular configuration of the previous section. It has no zero gaps, of course. Note however, that in this case the zero of potential is defined as the bottom of the well, instead of the top, so diagram 4.6 and diagram 4.10 are different.

Figure 4.8: Well width equal to one fifth the period

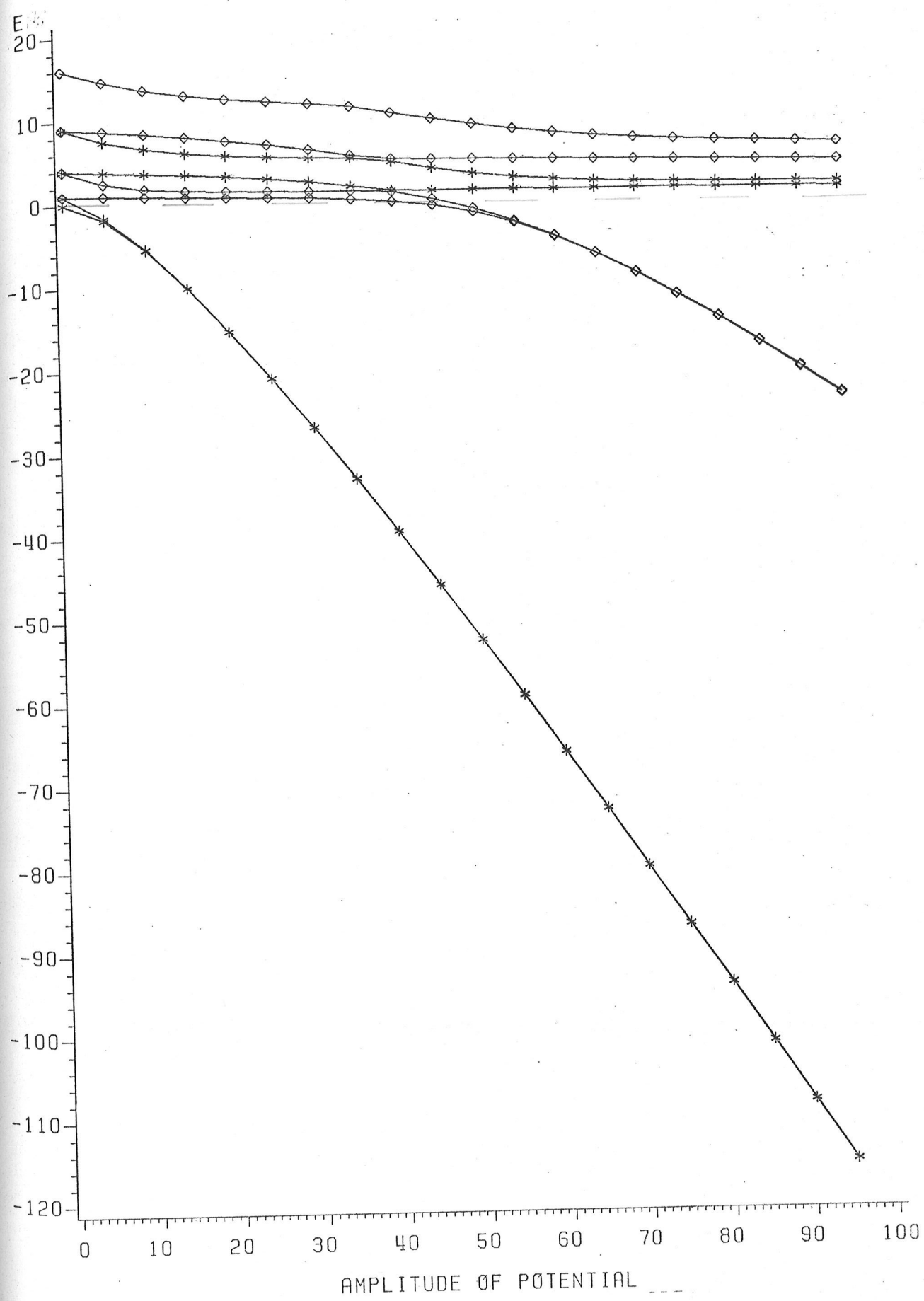


Figure 4.9: Well width equal to one half the the period

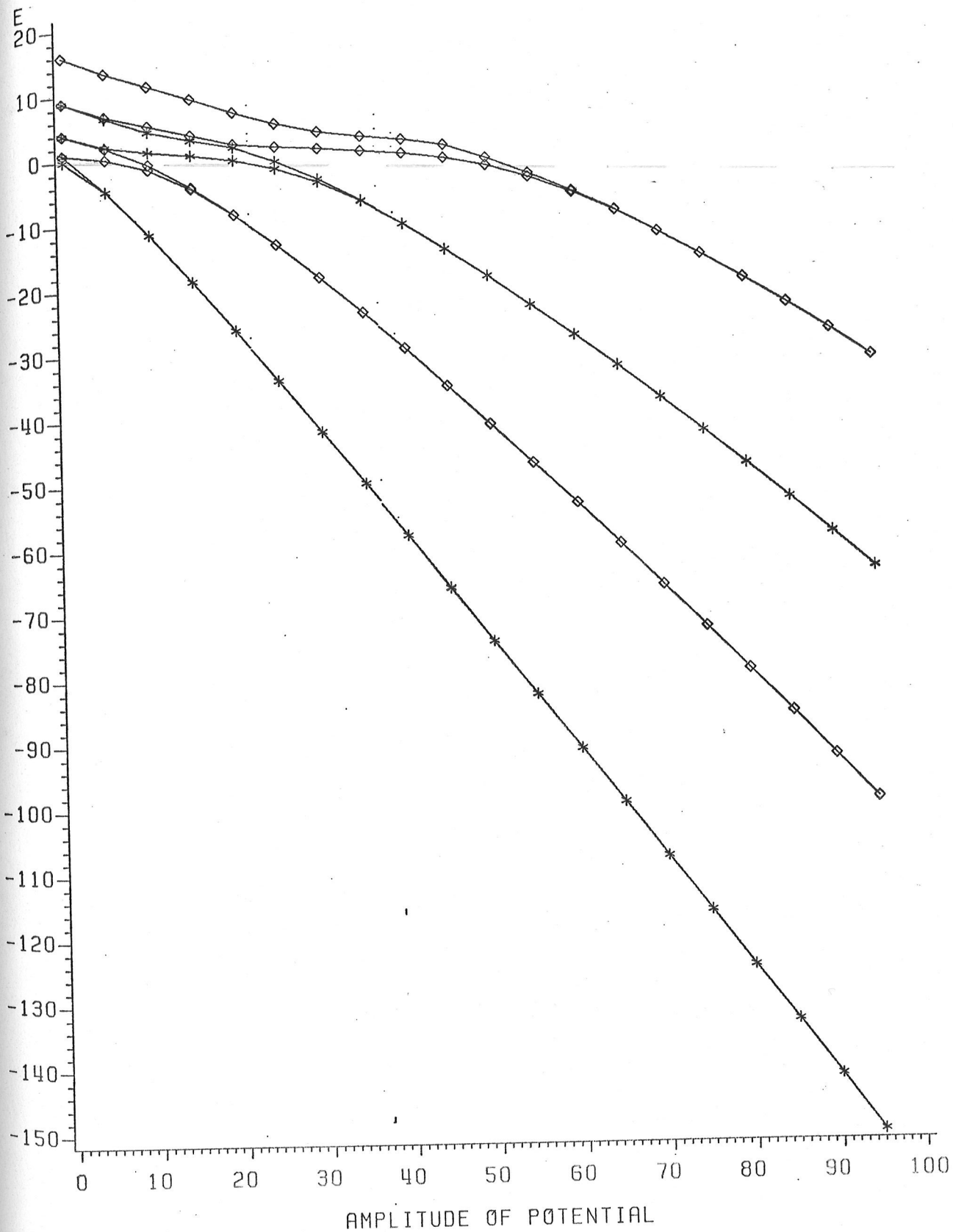
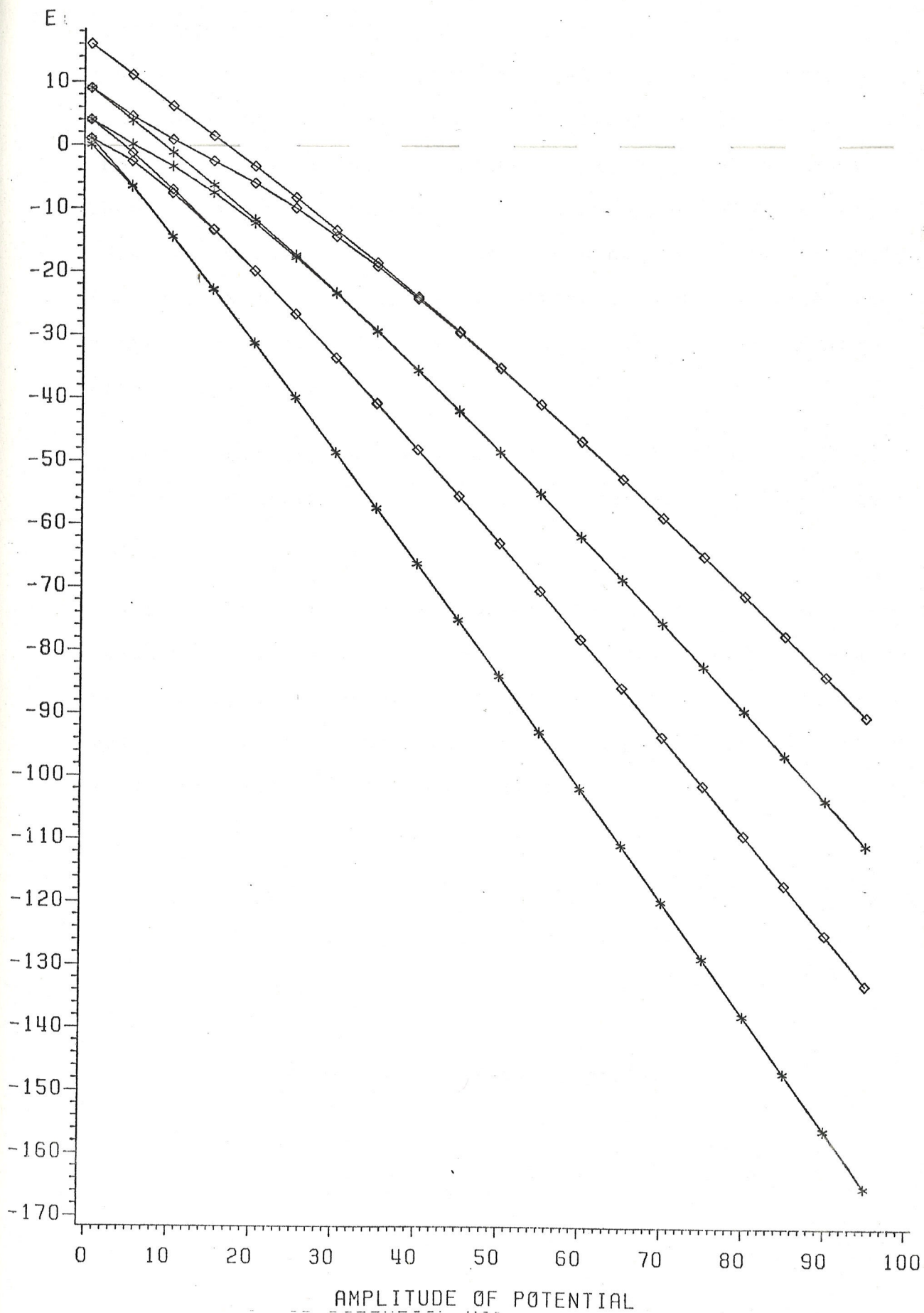


Figure 4.10: Plateau Vanishes



4.7 SUPERLATTICE POTENTIAL

Finally, the band structure of electrons in a superlattice representation is computed. A superlattice is a material where two layers of different materials are interwoven. They can occur as alloys, such as a copper-aluminum alloy (Sato and Toth, 1961), or they can be grown synthetically (Dohler, 1983). If the superlattice consists of a periodic array of two different materials, it is called a compositional superlattice.

For simplicity a compositional superlattice consisting of two Kronig-Penney potentials is studied here (see figure 4.1).

It has been observed (Landauer, 1981), that changing the relative sizes of well 1 and well 2 determines the existence of zero gaps. Apparently they appear when the well depth of well 1 is about the same as the well depth of well 2, for an (AB) superlattice (see figure 4.11).

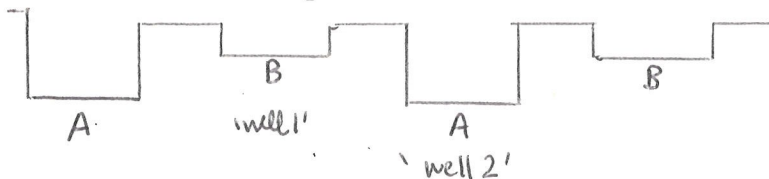


Figure 4.11: (AB) Superlattice

When well 1 is one half the size of well 2, a few zero gaps appear, as in figure 4.12. When well 1 has the same depth as well 2, similar to a simple Kronig-Penney well, there are, as predicted, vanishing band gaps. Finally, when well 1 is five times the size of well 2, the zero gaps disappear.

Finally, it should be noted that this potential has localized wells with a flat region in between. Thus, indeed, it shows vanishing band gaps.

Thus, the zero gaps appearing in the band structures studied seem to satisfy the above conditions.

Figure 4.12: Superlattice potential, well 2 = $1/2$ size of well 1

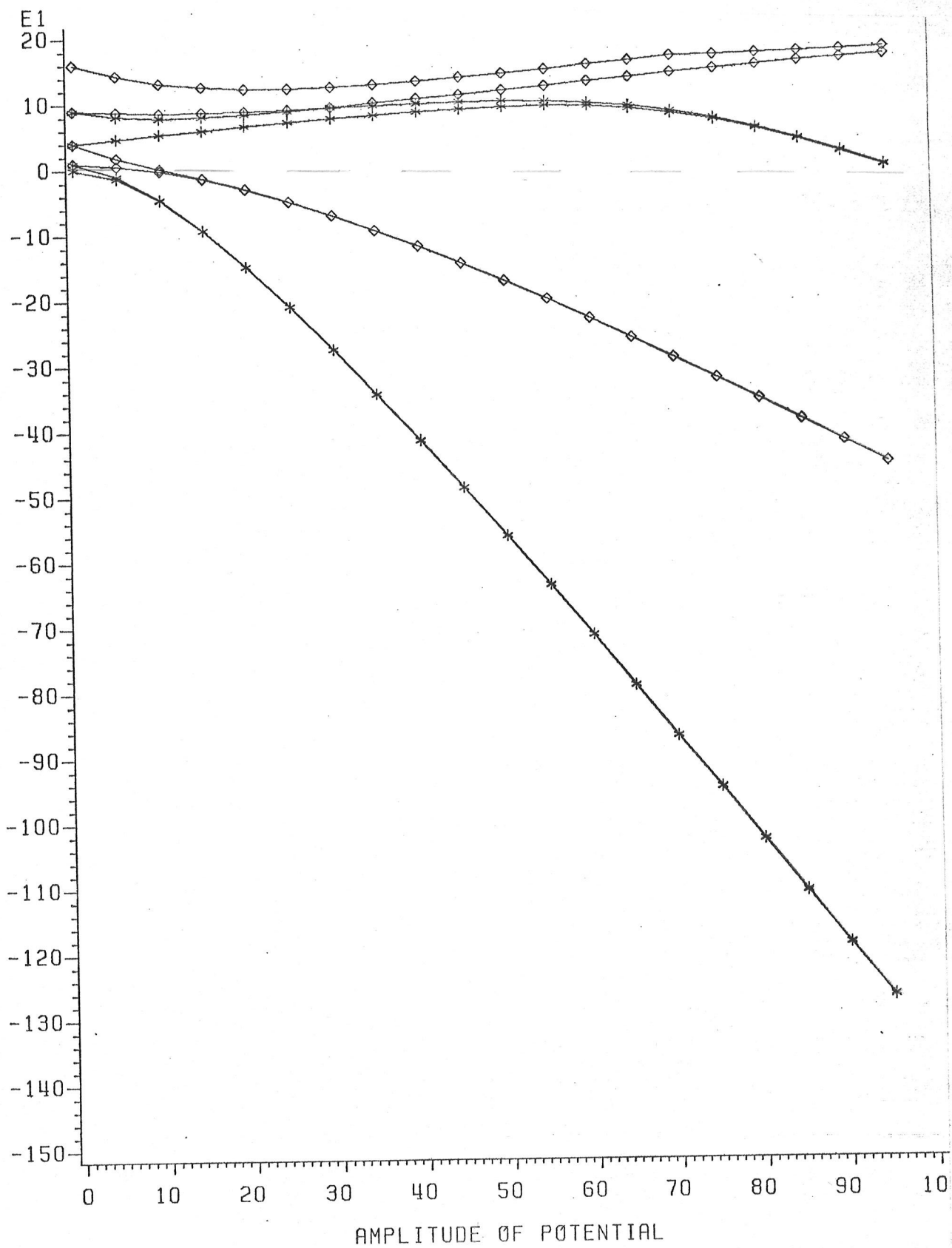


Figure 4.13: Superlattice potential, well 2 = size of well

1

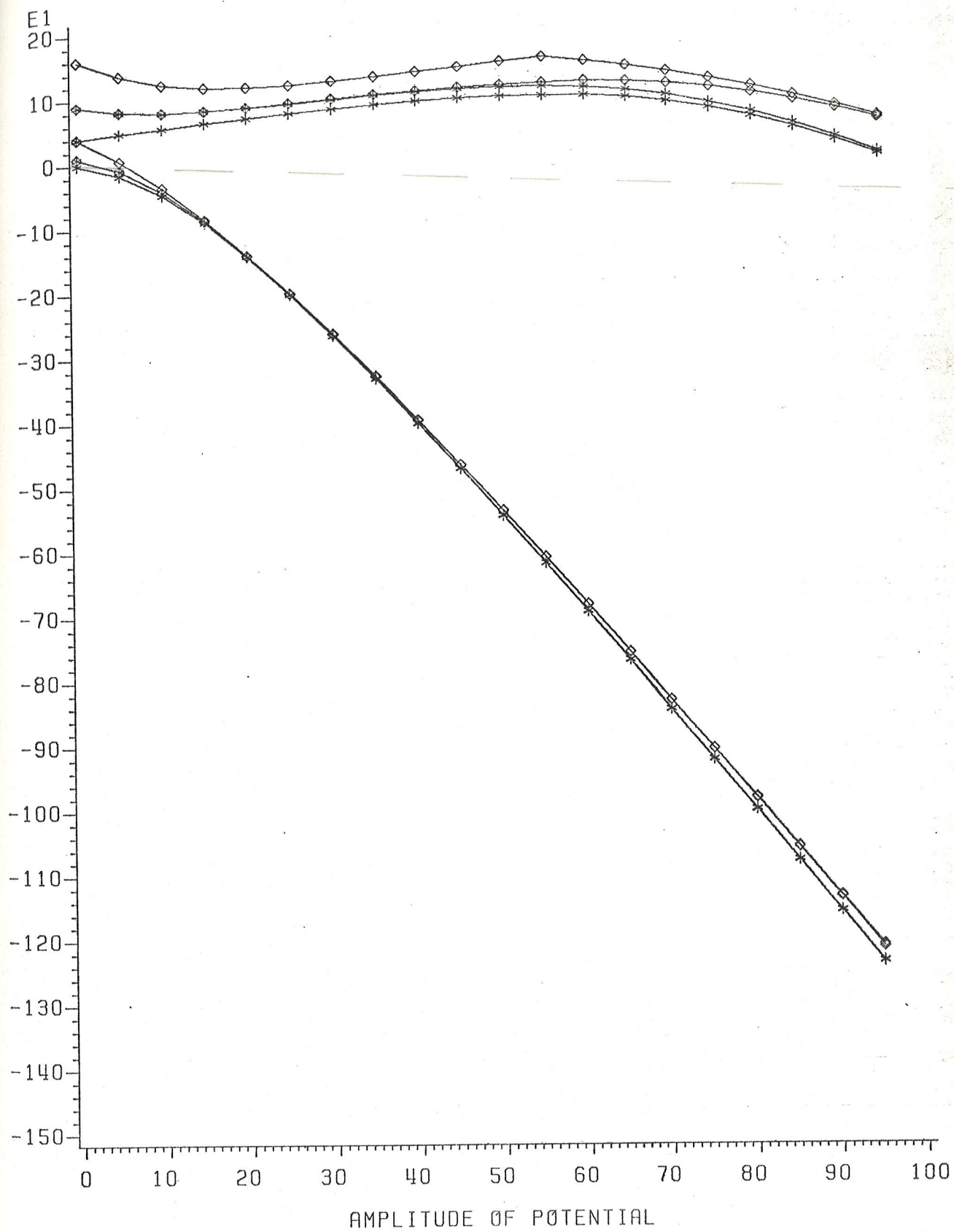
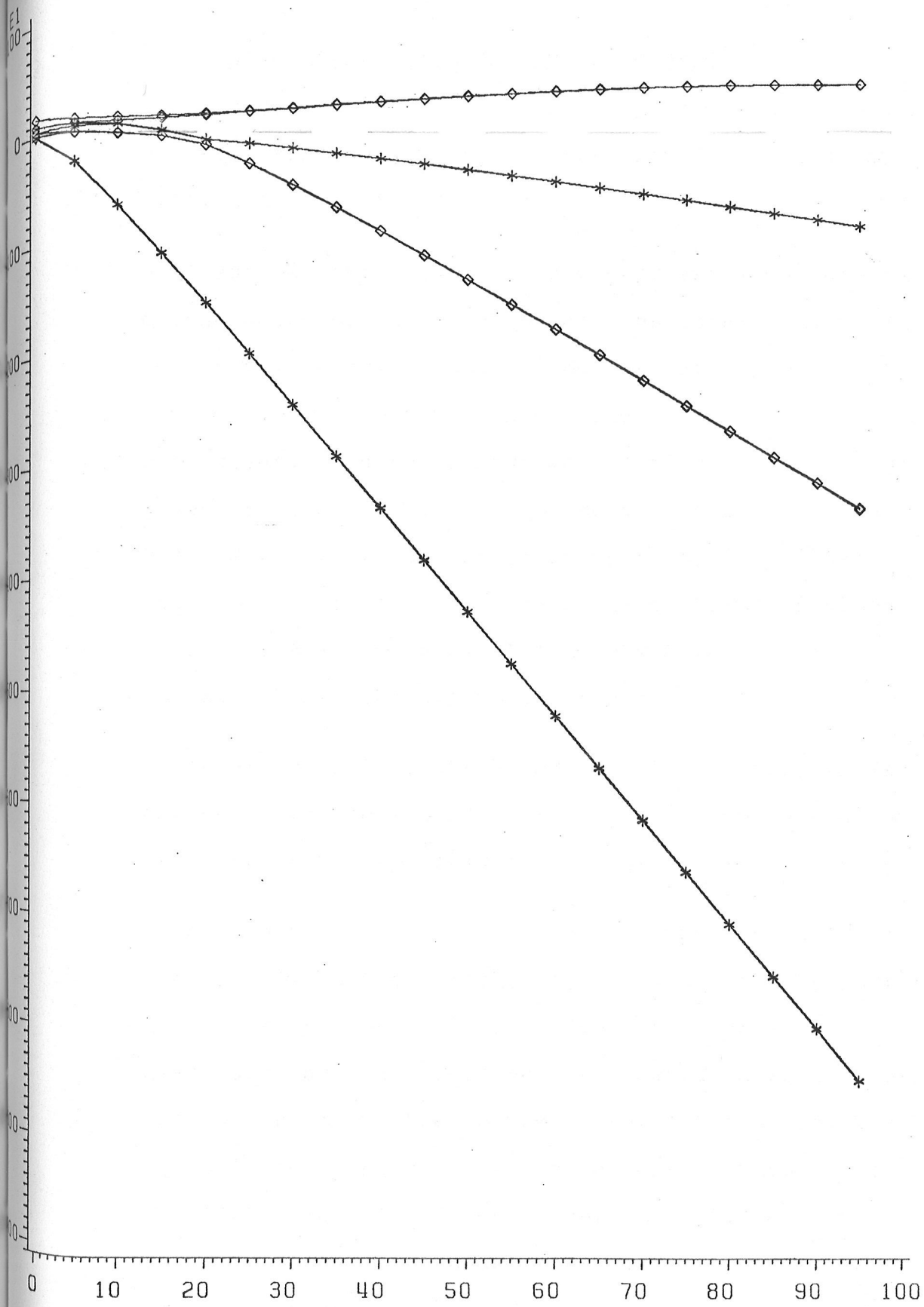


Figure 4.14: Superlattice potential, well 2 = five times
size of well 1



4.8 SOME EXPLANATION OF ZERO BAND GAPS

One can give conditions for the appearance of zero gaps, as we have seen, but to explain why they occur is a little more difficult.

These vanishing gaps are commonly explained as accidental degeneracies of Bloch Waves at the zone boundaries. The reason why there is such a degeneracy is not quite clear, but an argument may be constructed as follows. For a (2x2) approximation in the energy calculations, the energy gap is given by $\Delta E = 2|V_G|$ at the zone boundary (Ziman, 1979). Using more reciprocal lattice vectors, say (15x15), there would be additional potential energy terms influencing the size of the energy gap. If there were a cancellation of potential terms, the gap would be zero.

In general, it might be added, if symmetry is destroyed, degeneracies are lifted. Hence if the wells are not symmetric, the band gap would not vanish.

Alternately, one can examine the question of wave reflection. Recall that band gaps are explained by particle reflections at the Brillouin Zone Boundary. But remember also, that any wave incident on a medium does not reflect if the thickness of the medium is equal to an integral number of half wave lengths. In such a case, a wave propagating in the flat interstitial region between wells will not be scattered by the well (Lin and Smit, 1981). If there is no reflection, there is no band gap.

In summary, for particular values of a certain potential, band gaps disappear. This is a fundamental feature of band structure calculations, but it is widely overlooked (Landauer, 1981). Since one traditionally demonstrates band structure by Kronig-Penney wells which are not well localized, or by Mathieu potentials, zero gaps are not seen.

V

WAVEFUNCTIONS

Now that electron energies have been calculated, the next logical step is to calculate wavefunctions of electrons subject to given potentials. The expression for the wavefunction, as mentioned earlier, is

where α_{k-G} is the coefficient of the plane wave $e^{i(k-G)x}$.

$$\Psi_k(x) = \sum_k \alpha_{k-G} e^{i(k-G)x}$$

There is a wavefunction, of course, corresponding to each electronic energy state.

Computationally, it is quite easy to obtain the coefficients α , from the solutions of the algebraic equation (3). They are proportional to the eigenvector of the programmed determinant. There will an eigenvector, and hence a wavefunction for each energy eigenvalue.

The wavefunction can be studied as a function of wavevector k , for a fixed x , or as a function of position in the crystal, x , for a fixed k . Rather than exhibit the wavefunction Ψ , though, the electron probability, $|\Psi|^2$, or charge density, is presented. Alternately, a three dimensional plot of x, k , and probability amplitude could be plotted. Once the wavefunction is computed, the probability amplitude, or the charge density is easily obtained.

5.1 TEST WAVEFUNCTION

As a test of the wavefunction calculations, the wavefunctions were computed using the standard two by two approximation (Ziman, 1979). In this approximation, the electrons have a wavevector corresponding to the first Brillouin Zone.

In the (2x2) approximation, only two equations of (3) are used:

$$\begin{aligned} \{\varepsilon_k^0 - \varepsilon(k)\} \alpha_k + V_G \alpha_{k-G} &= 0 \\ V_{-G} \alpha_k + \{\varepsilon_{k-G}^0 - \varepsilon(k)\} \alpha_{k-G} &= 0 \end{aligned}$$

Assuming, though, that the potential energy, V_G , is small in comparison to the kinetic energy of the free electron.

The energies, for the sake of comparison, are given by

$$\varepsilon^\pm(k) = \frac{1}{2}(\varepsilon_k^0 + \varepsilon_{k-G}^0) \pm \frac{1}{2} \sqrt{\{(\varepsilon_k^0 - \varepsilon_{k-G}^0)^2 + 4|V_G|^2\}}$$

near $k=0$,

$$\varepsilon(k) \sim \varepsilon_k^0$$

near the zone boundary,

$$\varepsilon^-(\frac{1}{2}G) = \varepsilon_{\frac{1}{2}G}^0 - |V_G|$$

$$\varepsilon^+(\frac{1}{2}G) = \varepsilon_{\frac{1}{2}G}^0 + |V_G|$$

Thus the width of the energy gap at the zone boundary is $2|V_G|$. The general expression for the wavefunction, of course, is

$$\Psi_k(x) = \sum_G \alpha_{k-G} e^{i(\vec{k}-\vec{G}) \cdot \vec{r}}$$

for $k = G/2$, the zone boundary,

$$\Psi^- = \sqrt{2} \cos(\frac{1}{2}Gr)$$

$$\Psi^+ = \sqrt{2} \sin(\frac{1}{2}Gr)$$

Thus, $|\psi|^2$ is large near $x=0$, and at every other lattice site, with a maximum value of two.

Physically, this corresponds to the electrons being centred on atoms. In other words, the potential is an attractive potential.

Finally, it should be noted that the (2x2) approx is centred around the zone boundary.

Program Modification for (2x2) case

Since the program is set up for an odd number of reciprocal lattice vectors, corresponding to symmetry about the zone centre, a 'block' of the (3x3) matrix is taken.

$$\begin{bmatrix} t_1 & v_1 & v_2 \\ v_1 & t_0 & v_1 \\ v_2 & v_1 & t_1 \end{bmatrix}$$

Results

The wavefunctions in this (2x2) approximation were calculated for the Mathieu Potential with amplitude 0.1, and for $k=0, 1$.

For $k=0$, the zone centre, the probabilities oscillate about $|\psi|^2 = 1$, as in diagram 5.1.

For $k=1$, the zone boundary, the two wavefunctions represent standing waves. One probability amp is zero at $x=0$, whereas

the other one is a maximum, $|\Psi|^2 = 2$. The results are plotted in figure 5.2.

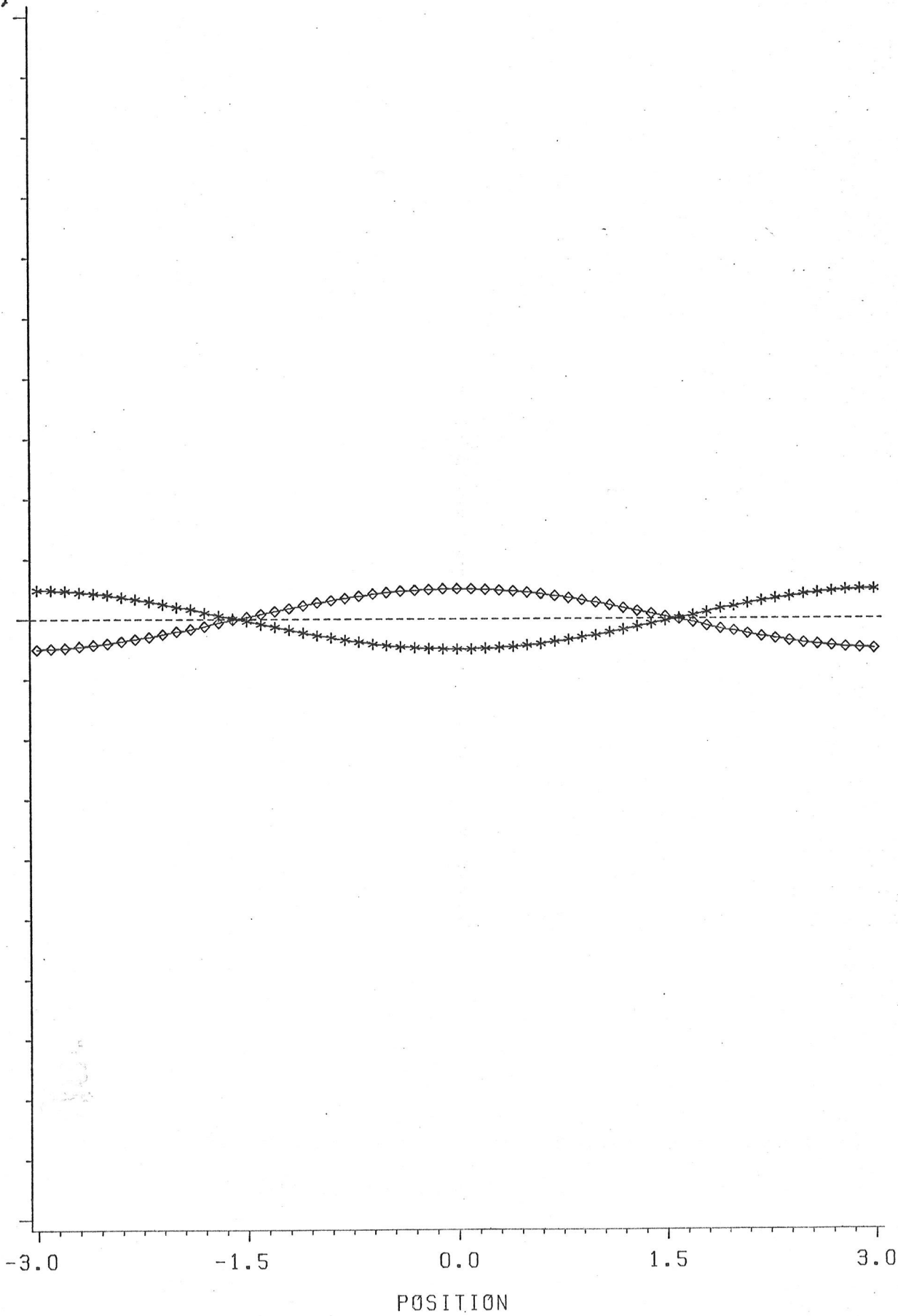
It must be noted that the (2x2) approximation is centred at the zone boundary, and cannot reproduce quadratic behavior of the bands at the zone centre (Loly and Bahurmuz, 1979). This two by two approximation is improved in the next section.

Figure 5.1: Probability density of electrons subject to
Mathieu Potential, $K=0$

(PROB)
2

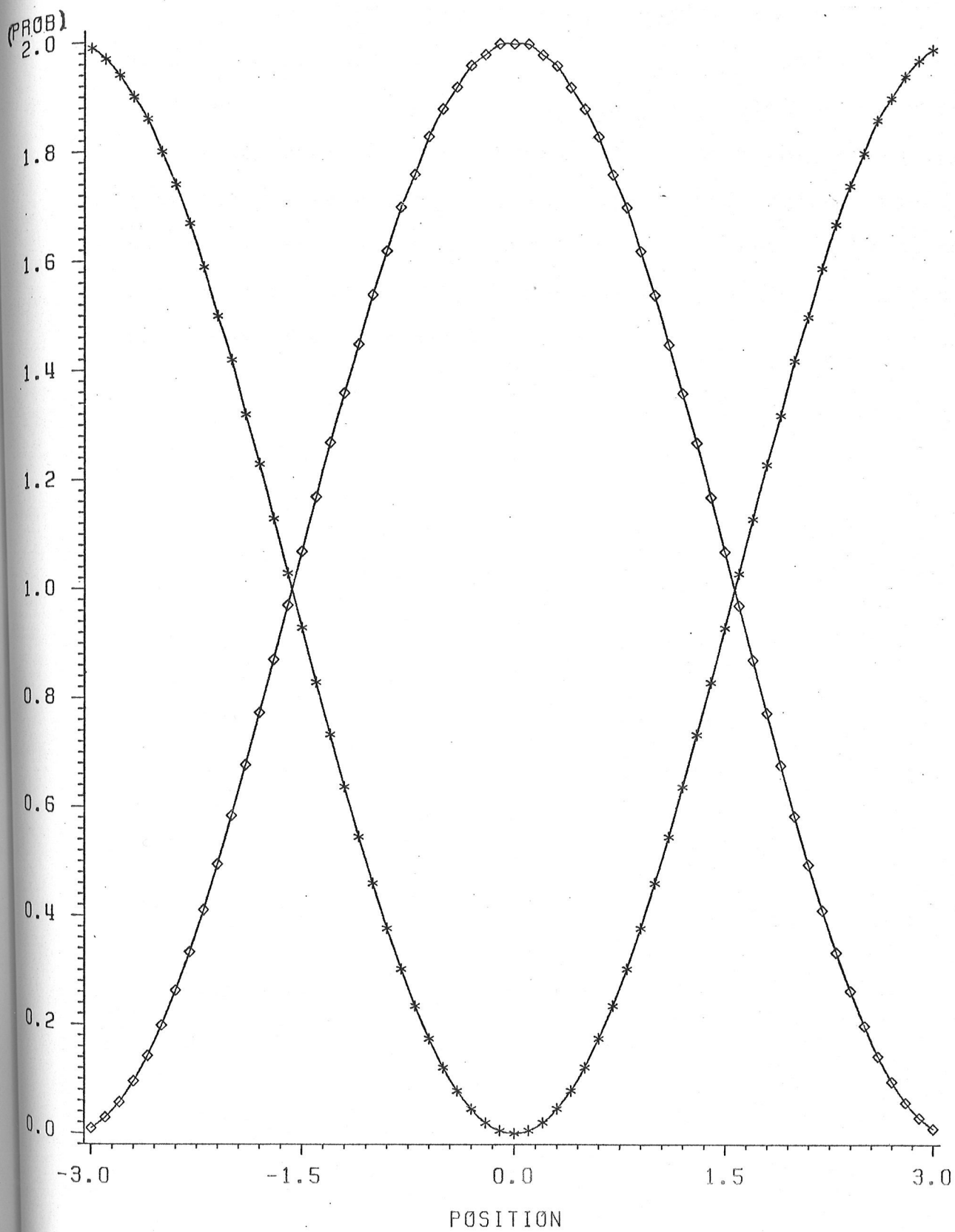
1

0



POSITION

Figure 5.2: Probability density of electrons subject to Mathieu Potential, $K=1$

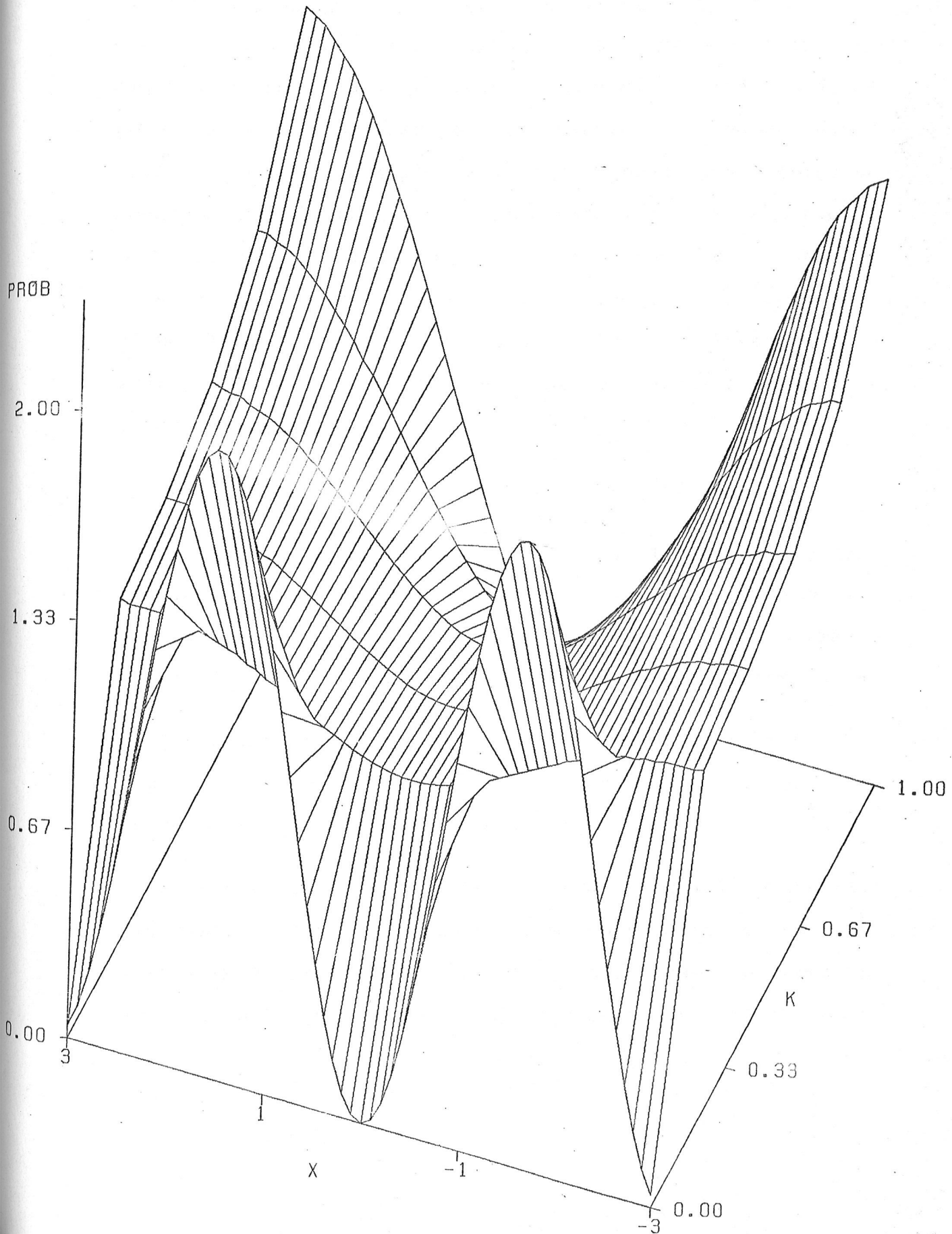


5.2 $|\Psi|^2$ FOR LOWEST BAND OF MATHIEU POTENTIAL

Next, a three dimensional plot of $|\Psi|^2$, x , and k is shown in figure 5.3. The probabilities were calculated in the (3x3) approximation, and correspond to the lowest energy eigenvalue. The probability amplitude, once again, shows a maximum at $x=2$ and a minimum at $x=0$. In this three dimensional plot, the variation of Probability amplitude with the wavevector k can be seen.

Figure 5.3: Three dimensional plot of $|\Psi|^2$, x , and k for an electron subject to a Mathieu Potential

PROBABILITY AMPLITUDES AS A FUNCTION OF K AND X



5.3 $|\Psi|^2$ FOR OTHER POTENTIALS USING (15X15) PLOT

Finally, the wavefunctions for electrons subject to the Kronig-Penney potential, triangular potential, the triangular potential with a plateau between the wells, and the superlattice potential are plotted. Each Probability density has been computed in the (15x15) approximation, with a period of π . The wavefunctions corresponding to the lowest three energy states are presented. They are labelled $|\Psi_1|^2$ for the probability density corresponding to the lowest energy state, $|\Psi_2|^2$ for the second energy state, and $|\Psi_3|^2$ for the third lowest energy state.

The results are presented on the next few pages.

For the Kronig-Penney potential, $|\Psi_1|^2$ is centred on zero, similar to the Mathieu potential in the (2x2) approximation, with $k=1$. The second probability density has maxima at about $\pm\pi/2$. The third probability density has maxima at $\pm\pi$.

For the triangular potential $|\Psi_1|^2$ is centred on $x=0$, rising to a maximum at $\pm\pi$. $|\Psi_2|^2$ is a maximum at $x=0$, and falls to zero at $\pm\pi$, whereas $|\Psi_3|^2$ oscillates.

When the plateau is added to the triangular potential, $|\Psi_1|^2$ flattens out, being small from $x=0$ to about $x=\pm\pi/2$, then rising to a max at about π . $|\Psi_2|^2$ is also lower in value, but is still a maximum at $x=0$. $|\Psi_3|^2$ once again oscillates.

Finally, the probability amplitudes in the superlattice are similar to those of the triangular potential with a plateau. $|\Psi_1|^2$ is a maximum at $x=0$, and falls to a minimum at about $x = \pm\pi$. $|\Psi_2|^2$ is zero at $x=0$ and rises to a maximum at $x = \pm\pi$. $|\Psi_3|^2$ once again oscillates.

Figure 5.4: Probability amplitudes of electrons subject to a Kronig-Penney potential

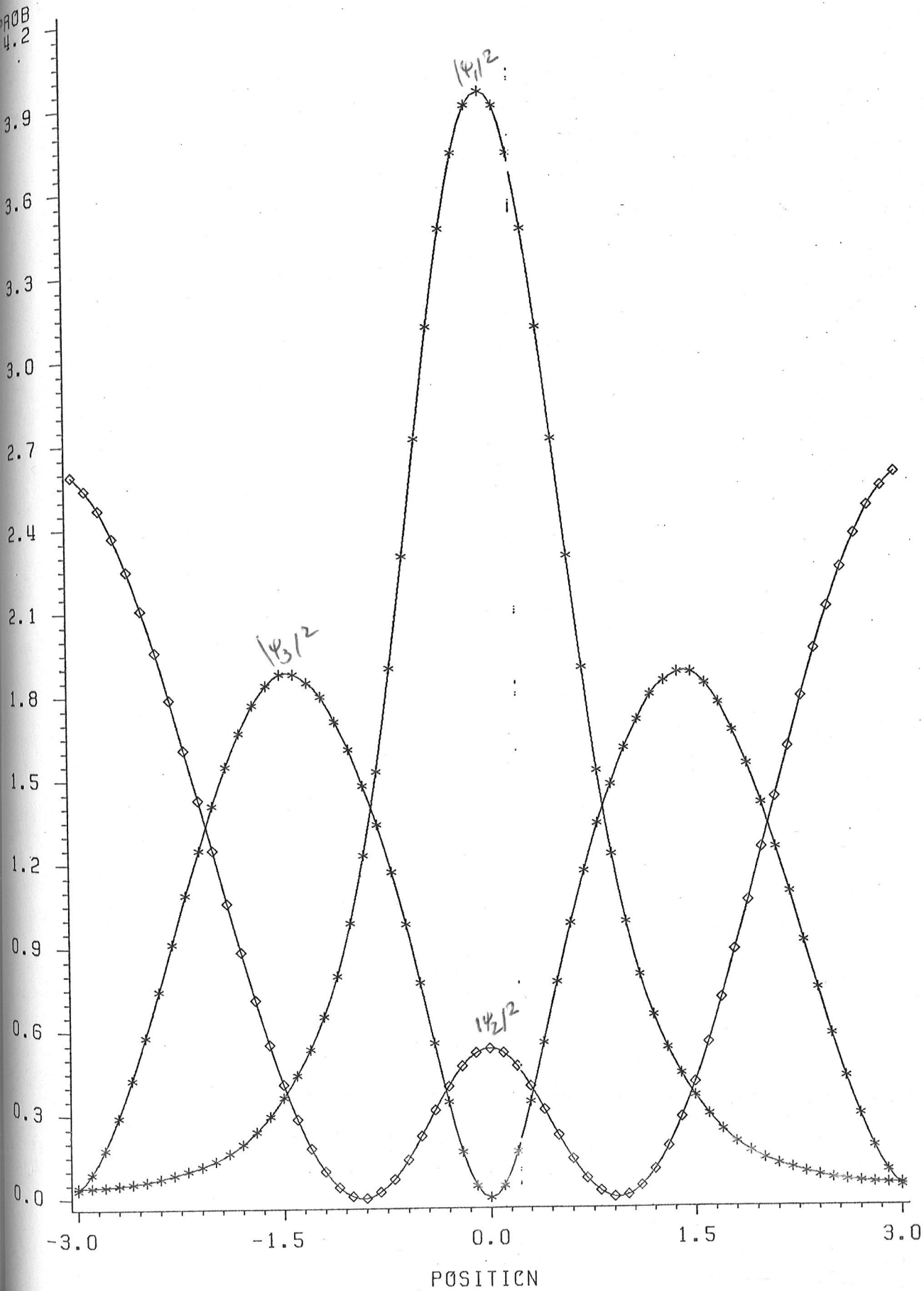


Figure 5.5: Probability amplitudes of electrons subject to
a Triangular Potential

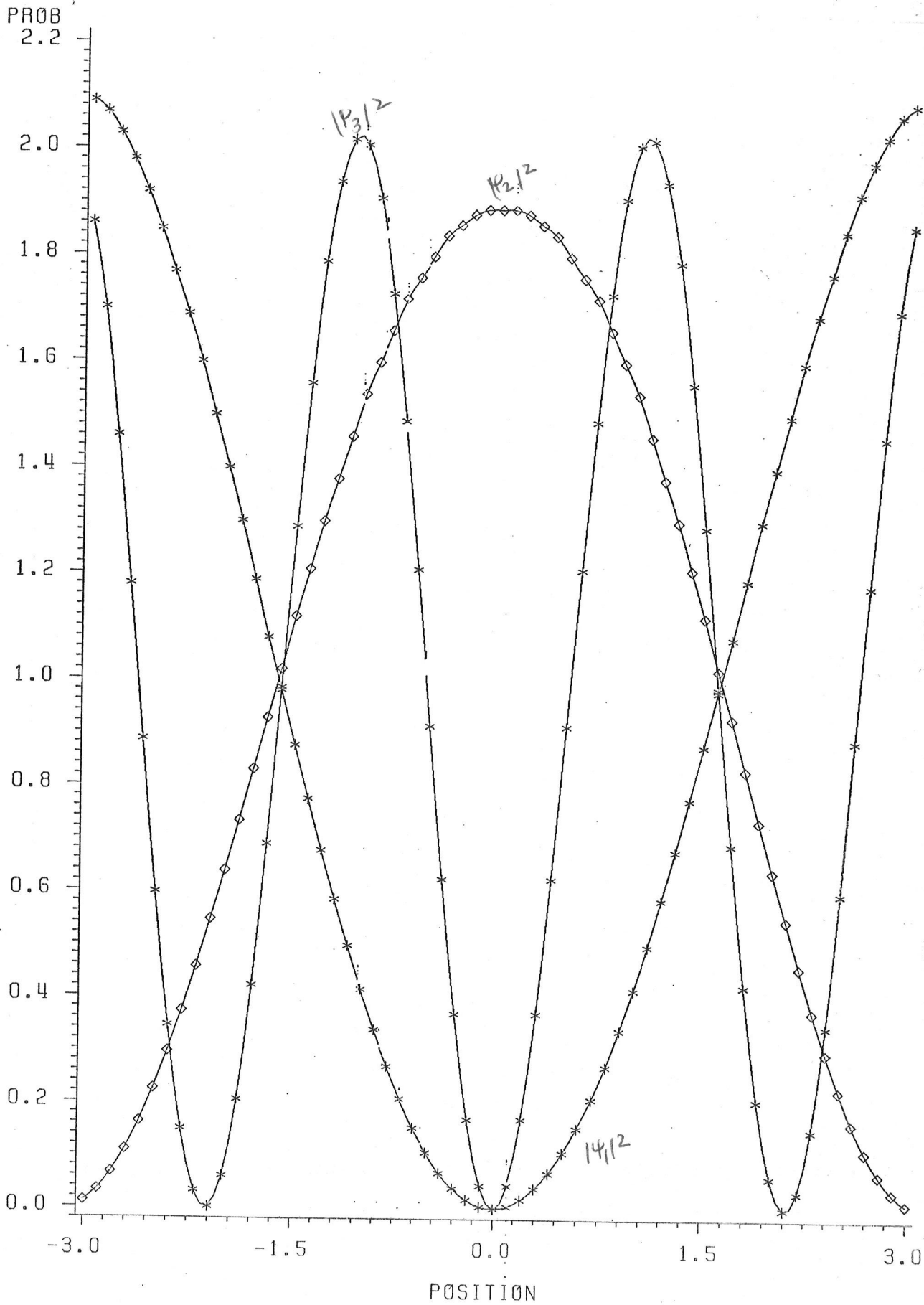
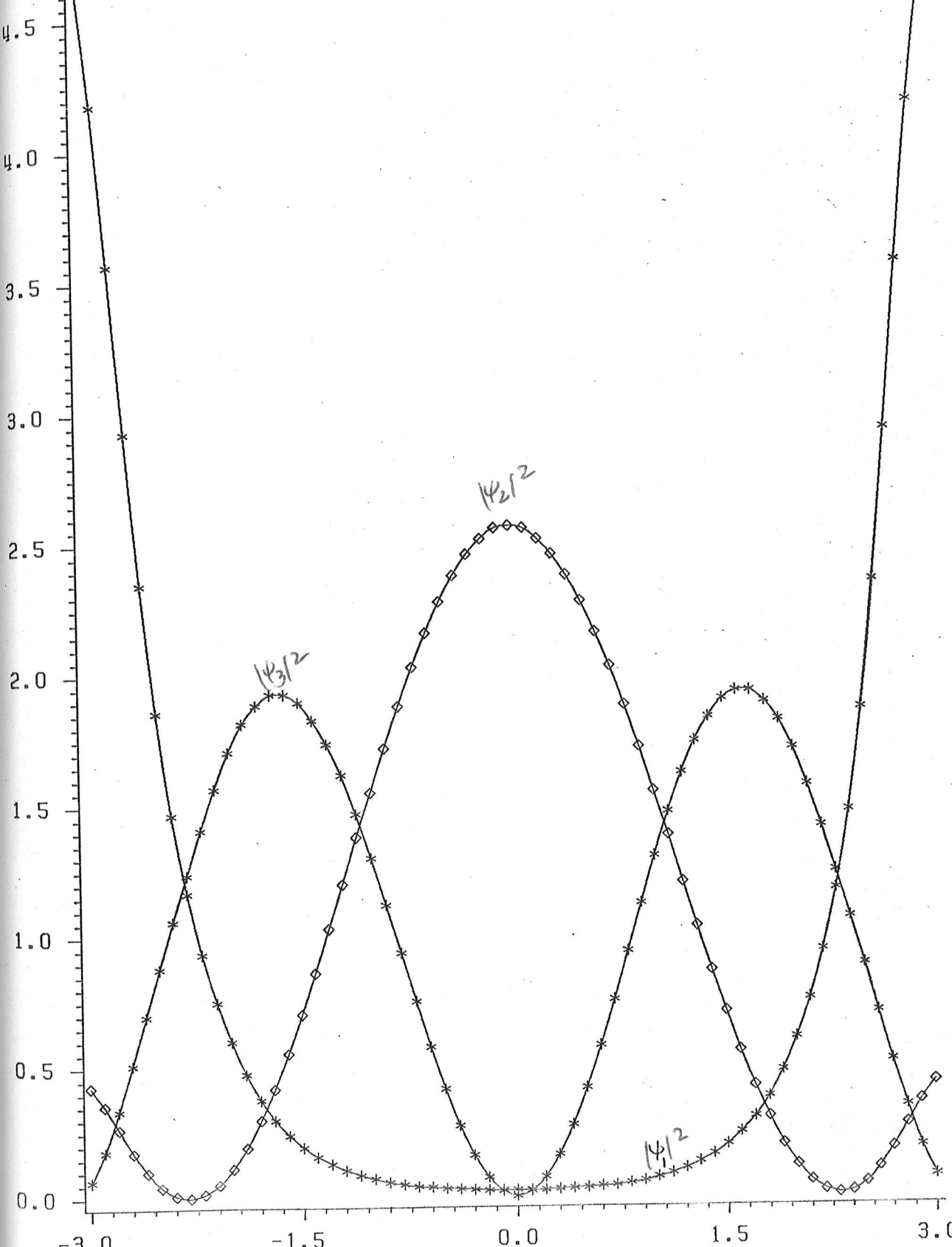


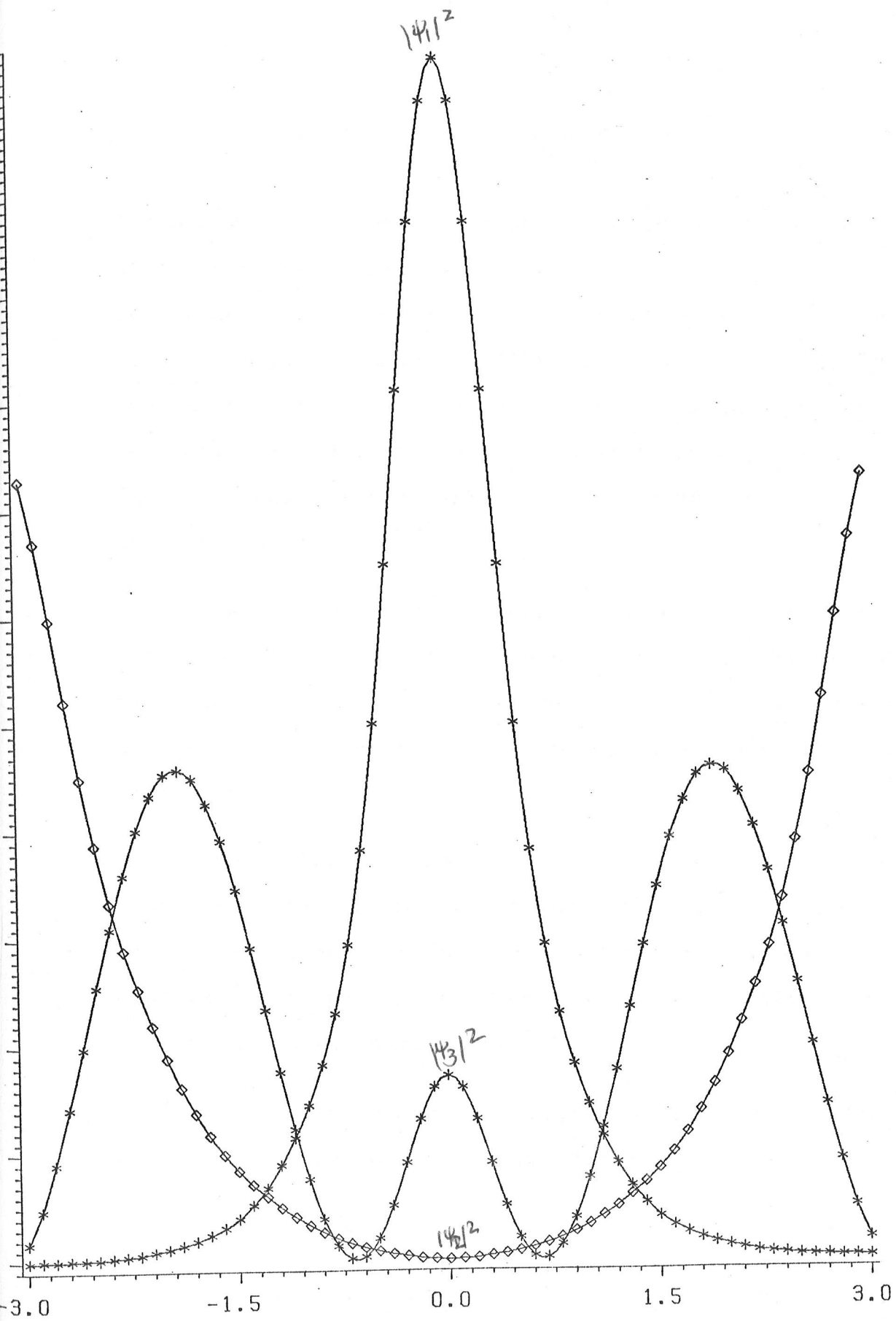
Figure 5.6: Probability amplitudes of electrons subject to a Triangular Potential with a Plateau

PROB



POSITION

Figure 5.7: Probability amplitudes of electrons subject to a Superlattice Potential



VI

CONCLUSIONS

The PWD Method has been described and used to find the energies and wavefunctions of electrons subject to certain interesting periodic potentials. As an extension of earlier studies (Loly and Bahurmuz 1979,1980,1981) a study of ionized states has been added to the low-lying ones treated earlier. In addition to the study of energy bands, wavefunction calculations exhibited as charge densities have been initiated.

The PWD Method has once again proved to be an efficient and accurate approach as demonstrated by the study of the triangular potential. The emphasis has then been to explore the energy spectra of various potentials, with results exhibited graphically.

In the ionized states of the Kronig Penney and other potentials, the phenomenon of vanishing gaps has been examined. This phenomenon has received renewed attention in recent years, in particular from Lin and Smit (1981) and other investigators who have quoted them.

Interestingly, a search of the literature shows that zero gaps, especially for the Kronig-Penney potential, have been

observed from the earliest days of the modern theory of solids. They were noted in Strutt's studies (1928), which even predates the studies of Bloch (1928).² It is also interesting to note that Lin and Smit (1981) and Strandberg (1982) do not even trace zero gaps back to Allen (1953), who made the clearest study.

Lin and Smit (1981) also make an unsubstantiated comment to the effect that a perfectly flat plateau between the wells is not necessary for zero gaps to occur. With the PWD approach and the diffraction interpretation of it (Loly and Bahurmuz, 1980), one can see the truth of this statement, because the truncated (15x15) determinant cannot produce a perfectly flat plateau.

Zero gaps also appear to be a more general phenomenon. They were found by Loly (private communication) in calculations for plasmons in layered materials, though this was not the primary feature of concern in the initial report (Caille et al, 1981). Since a Kronig-Penney charge density profile with variable rectangularity was used in a formulation equivalent to the present bandstructure problem, one can now identify the origin of those previously puzzling gap disappearances.

² For a brief account of this piece of history, see the paper by Loly and Bahurmuz (1979).

One point for further study, though, concerns the conditions outlined for the occurrence of zero gaps. It appears that the wells must be "localized" for these vanishing gaps to occur. It was found empirically, for example, that for certain potentials a well width one fifth the period produced zero band gaps, but a well width one half the period did not. Further study is needed to establish a criterion for zero gaps.

One strength of the PWD approach is that it is readily adapted to higher dimensions, as demonstrated by a two and three dimensional generalization of the Mathieu problem (Bahurmuz and Loly, 1979). Clearly, a two and three dimensional counterpart of the Kronig-Penney potential can be treated. This extension to higher dimensions offers interesting possibilities for studying dimensional cross-over effects, similar to zero gaps in one dimension.

Finally, the initial wavefunction calculations were restricted to charge density calculations only. They could be extended to calculations of matrix elements arising in the dielectric susceptibility $\chi(q, \omega)$ (Ziman, 1979), or other calculations involving the electronic wavefunction in a crystal.

In conclusion, the PWD Method continues to be an efficient method of calculating the bandstructure and wavefunctions of electrons subject to periodic one-dimensional potentials.

VII
BIBLIOGRAPHY

BIBLIOGRAPHY

- Allen, G. "Band Structure of One-Dimensional Crystals with Square Well Potentials." Physical Review. 91(August 1953): 531-533.
- Ashbaugh, Mark, and Morgan, John D. "Remarks on Turschner's eigenvalue formula." Journal of Physics A. 14(April 1981): 809-819.
- Bahurmuz, A. A. and Loly, P.D. "Model Bandstructure Calculations." American Journal of Physics. 49(July 1981): 675-680.
- Bube, Richard H. Electrons in Solids. New York: Academic Press, 1981.
- Caille, A., et al. "The Crossover from Two-Dimensional to Three-Dimensional Plasmon Behavior in Layered Systems." Solid State Communication. 41(January 1982): 119-122.
- Clarke, R.D. and Martin, D.J. "Electron Energy Bands in a One-dimensional Periodic Potential" in Physics Programs edited by A.D. Boardman. New York: John Wiley and Sons, Limited, 1980.
- Dohler, Gottfried H. "Solid State Superlattices." Scientific American. 249(November 1983): 144-151.
- Gossard, A.C., et al. "Molecular Beam Epitaxial Growth and Electrical Transport of Graded Barriers for Nonlinear Current Conduction." Journal of Vacuum Science and Technology. 20(March 1982): 694:700.
- Herring, Conyers. "Accidental Degeneracies in the Energy Bands of Crystals." Physical Review. 52(August 1937): 365-373.
- International Mathematical and Statistical Library, Inc. "EIGRS." Houston, Texas.
- Kittel, C. Introduction to Solid State Physics. New York: John Wiley and Sons, Inc., 1968.
- Koelling, D.D. "Self-Consistent Energy Band Calculations." Reports on Progress in Physics. 44(February 1981): 139-212.

- Kolbas, R.M. and Holonyak Jr., N. "Man-made quantum wells: A new perspective on the finite square well problem." American Journal of Physics. 52(May 1984): 431-437.
- Kronig, R. de L., and Penney, W.G. "Quantum Mechanics of Electrons in Crystal Lattices." Proceedings of the Royal Society of London. A130(February 1931): 499-513.
- Landauer, Rolf. "Pyroelectricity and Rezolectricity are Not True Volume Effects." Solid State Communications. 40(December 1981): 971-974.
- Lieb, Elliot H., and Mattis, Daniel C. Mathematical Physics in One-Dimension. New York: Academic Press, 1966.
- Lin, S.T. and Smit, J. "Zero Energy Gaps for One-Dimensional Periodic Potentials." American Journal of Physics. 48(March 1980): 193-196.
- Lippmann, B.A. "Surface States in Crystals." Annals of Physics. 2(July 1957): 16-27.
- Loly, P.D., and Bahurmuz, A.A. "Finite Diffraction Models for Electron Bandstructures." Annals of Physics. 129(July 1979): 120-144.
- Loly, P.D., and Bahurmuz, A.A. "A Comparitive Study of Energy Bands in Kronig-Penney and Mathieu Potentials." Physica B. 100(April 1980): 29-34.
- Miller, R.C. et al. "Parabolic quantum wells with the GaAs-Al Ga As system." Physical Review. 29(March 1984): 3740-3743.
- Pincherle, L. "Band Structure Calculations in Solids." Reports on Progress in Physics. XXIII(1960): 355-394.
- Pol, B. van der., and Strutt, M.J.O. "On the Stability of the Solution of Mathieu's Equation." Philosophical Magazine. 5(January 1928): 18-38.
- Sato, Hiroshi and Toth, Robert S. "Effect of Additional Elements on the Period of CuAuII and the Origin of the Long-Period Superlattice." Physical Review. 124(December 1961): 1833-1847.
- Scarf, Frederick L. "New Soluble Energy Band Problem." Physical Review. 112(November, 1958): 1137-1140.
- Strandberg, M.W.P. "Zero-energy gaps for deep one-dimensional potentials." American Journal of Physics. 50(December 1982): 1168-1169.
- Strutt, M.J.O. "Zur Wellenmechanik des Atomgitters." Annalen der Physik. 86(June 1928): 319-324.

- Vigneron, J.P., and Lambin, Ph. "A continued fraction approach to the numerical determination of one-dimensional band structures." Journal of Physics A. 12(November 1979): 1961-1970.
- Wetzel Jr., Grover C. "Calculation of the energy-band structure of the Kronig-Penney model using the nearly-free and tightly-bound electron approximations." American Journal of Physics 46(July 1978): 714-720.
- Wille, L., Verschelde, P., and Phariseau, P. "A new solvable one-dimensional crystal model." Journal of Physics A. 16(1983): L771-L775.
- Ziman, J.M. "The Calculation of Bloch Functions." Solid State Physics. 26(1971): 1-101.
- Ziman, J.M. Principles of the Theory of Solids. London: Cambridge University Press, 1979.

VIII

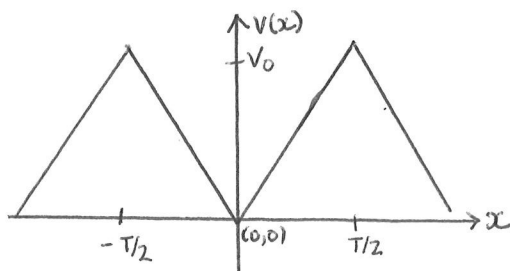
APPENDIX

For an even function, $V(x)=V(-x)$, the expression for the Fourier series is well known and given by

$$V(x) = a_0/2 + \sum_n a_n \cos(nwx)$$

$$a_n = \frac{4}{T} \int_0^{T/2} f(x) \cos(nwx) dx \quad w = 2\pi/T \quad T = \text{the period}$$

The Fourier series for the potentials studied are now derived.

8.1 TRIANGULAR POTENTIAL

$$V(x) = \begin{cases} \frac{2V_0}{T}x & 0 \leq x \leq \frac{T}{2} \\ -\frac{2V_0}{T}x & -\frac{T}{2} \leq x \leq 0 \end{cases}$$

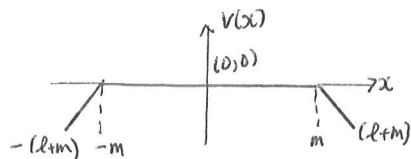
$$a_0 = \frac{4}{T} \int_0^{T/2} \frac{2V_0}{T} x dx = \frac{4}{T} \cdot \frac{2V_0}{T} \left(\frac{x^2}{2} \right) \Big|_0^{T/2} = V_0$$

$$\begin{aligned} a_n &= \frac{4}{T} \int_0^{T/2} \frac{2V_0}{T} x \cos(n\omega_0 x) dx = \frac{4}{T} \cdot \frac{2V_0}{T} \left[\frac{\cos(n\omega_0 x)}{(n\omega_0)^2} + \frac{x \sin(n\omega_0 x)}{(n\omega_0)} \right] \Big|_0^{T/2} \\ &= \frac{8V_0}{T^2} \left[\frac{\cos\left(\frac{n\omega_0 T}{2}\right)}{(n\omega_0)^2} + \frac{T/2 \cdot \sin\left(\frac{n\omega_0 T}{2}\right)}{n\omega_0} - \frac{1}{(n\omega_0)^2} \right] \end{aligned}$$

Noting that $\omega_0 = \frac{2\pi}{T}$ and $\cos\left(\frac{n\omega_0 T}{2}\right) = \cos(n\pi) = (-1)^n$
 $\sin\left(\frac{n\omega_0 T}{2}\right) = \sin(n\pi) = 0$

$$a_n = \frac{2V_0}{n^2\pi^2} [(-1)^n - 1]$$

$$V(x) = \frac{V_0}{2} + \frac{2V_0}{\pi^2} \left(\sum_{n=1}^{\infty} \frac{[(-1)^n - 1]}{n^2} \right) \cos\left(\frac{2n\pi}{T}\right)x$$

8.2 TRIANGULAR POTENTIAL WITH PLATEAU

$$V(x) = \begin{cases} \frac{V}{l} (x+m) & -(l+m) \leq x \leq -m \\ 0 & -m \leq x \leq 0 \\ 0 & 0 \leq x \leq m \\ \frac{V}{l} (-x+m) & m \leq x \leq (l+m) \end{cases}$$

$$a_0 = \frac{4}{T} \int_0^{T/2} V(x) dx = \frac{4}{2(l+m)} \int_m^{l+m} \frac{V}{l} (-x+m) dx = \frac{2}{(l+m)} \frac{V}{l} \left[-\frac{x^2}{2} + mx \right]_m^{l+m}$$

$$a_0 = \frac{-Vl}{(l+m)}$$

$$\begin{aligned} a_n &= \frac{2}{(l+m)} \frac{V}{l} \int_m^{l+m} (-x+m) \cos n\omega x dx = \frac{2V}{l(l+m)} \left\{ - \left[\frac{\cos n\omega x}{(n\omega)^2} + \frac{x \sin n\omega x}{(n\omega)} \right] + m \left[\frac{\sin n\omega x}{n\omega} \right] \right\}_m^{l+m} \\ &= \frac{2V}{l(l+m)} \left\{ - \frac{\cos n\omega(l+m)}{n\omega^2} - \frac{l \sin n\omega(l+m)}{n\omega} + \frac{\cos n\omega m}{(n\omega)^2} \right\} \end{aligned}$$

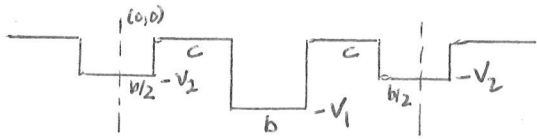
noting that $n\omega = \frac{n\pi}{(l+m)}$

$$\begin{aligned} \cos n\omega(l+m) &= \cos n\pi = (-1)^n \\ \sin n\omega(l+m) &= \sin n\pi = 0 \end{aligned}$$

$$a_n = \frac{2V(l+m)}{l(n\pi)^2} \left[(-1)^{n+1} + \cos \left(\frac{n\pi m}{(l+m)} \right) \right]$$

$$V(x) = \frac{-Vl}{2(l+m)} + \left\{ \frac{2V(l+m)}{l(n\pi)^2} \left[(-1)^{n+1} + \cos \left(\frac{n\pi m}{(l+m)} \right) \right] \right\} \cos \left(\frac{2n\pi}{T} \right) x$$

8.3 SUPERLATTICE POTENTIAL



$$V(x) = \begin{cases} -V_2 & 0 \leq x \leq b/2 \\ -V_1 & b/2+c \leq x \leq \frac{3b}{2}+c \\ -V_2 & \frac{3b}{2}+c \leq x \leq 2(b+c) \end{cases}$$

$$a_n = \frac{2}{T} \int_0^T f(x) \cos n\pi x dx$$

$$T = 2(b+c) = 2a \quad a = (b+c)$$

$$\omega = \frac{2\pi}{T} = \frac{\pi}{a}$$

$$a_n = \frac{1}{a} \left\{ \int_0^{b/2} -V_2 \cos(n\pi x) dx - V_1 \int_{b/2+c}^{3b/2+c} \cos(n\pi x) dx - V_2 \int_{3b/2+c}^{2a} \cos(n\pi x) dx \right\}$$

$$= \frac{1}{n\pi a} \left\{ -V_2 \sin(n\pi x) \Big|_0^{b/2} - V_1 \sin(n\pi x) \Big|_{b/2+c}^{3b/2+c} - V_2 \sin(n\pi x) \Big|_{3b/2+c}^{2a} \right\}$$

$$= \frac{a}{n\pi} \cdot \frac{1}{a} \left\{ -V_2 \sin\left(\frac{n\pi b}{2a}\right) - V_1 \sin\left(\frac{n\pi(3b/2+c)}{a}\right) + V_1 \sin\left(\frac{n\pi(b/2+c)}{a}\right) \right. \\ \left. - V_2 \sin\left(\frac{n\pi(2a)}{a}\right) + V_2 \sin\left(\frac{n\pi(3b/2+c)}{a}\right) \right\}$$

$$= \frac{1}{n\pi} \left\{ -V_2 \sin\left(\frac{n\pi b}{2a}\right) - V_1 \sin\left[\frac{n\pi(3b/2+c)}{a}\right] + V_1 \sin\left[\frac{n\pi(b/2+c)}{a}\right] \right. \\ \left. + V_2 \sin\left[\frac{n\pi(3b/2+c)}{a}\right] \right\}$$

$$a_0 = \frac{1}{a} \left\{ \int_0^{b/2} -V_2 dx - \int_{b/2+c}^{3b/2+c} V_1 dx + \int_{3b/2+c}^{2(b+c)} -V_2 dx \right\}$$

$$= \frac{1}{a} \left\{ -V_2 \left(\frac{b}{2}\right) - V_1(b) - V_2 \left(\frac{b}{2}\right) \right\}$$

$$= -\frac{b}{b+c} \{ V_1 + V_2 \}$$

$$V(x) = \frac{-b}{2(b+c)} (V_1 + V_2) + \left\{ \sum_{n=1}^{\infty} \frac{1}{n\pi} \left\{ -V_2 \sin\left(\frac{n\pi b}{2a}\right) - V_1 \sin\left[\frac{n\pi(3b/2+c)}{a}\right] \right. \right. \\ \left. \left. + V_1 \sin\left[\frac{n\pi(b/2+c)}{a}\right] + V_2 \sin\left[\frac{n\pi(3b/2+c)}{a}\right] \right\} \right\} \cos\left(\frac{2n\pi}{T}\right)x$$